Interfacial space charge and capacitance in ionic crystals: Intrinsic conductors

J. Ross Macdonald

Department of Physics and Astronomy, University of North Carolina, Chapel Hill, North Carolina 27514

Donald R. Franceschetti

Department of Physics, Memphis State University, Memphis, Tennessee 38152

Alfred P. Lehnen

Department of Physics and Astronomy, University of North Carolina, Chapel Hill, North Carolina 27514
(Received 27 May 1980; accepted 24 July 1980)

The conventional theory of surface charge and distributed space charge in single crystals exhibiting Frenkel or Schottky disorder is generalized in several ways. First we generalize the usual continuum theory of the diffuse double layer in the crystal by adopting a lattice gas model which restricts the mobile charges to a fixed number of lattice sites. The lattice gas activities can be used in both zero and nonzero current situations and are shown to be consistent with a three-dimensional generalization of ordinary Langmuir adsorption. The substantial effects of the resulting limit on concentrations in accumulation regions are examined and shown to be particularly important in high bias situations and in materials in which the bulk equilibrium charge densities are very high. Second, we take explicitly into account the physical separation between the plane of the surface charges, which balance the bulk space charge, and the first normal lattice plane of the crystal and show that under most conditions of interest this separation modifies the earlier surface potential results of Poeppel and Blakely substantially. We also show that the thermodynamically generated equilibrium relation between surface charge density and surface potential is itself just a form of the Langmuir adsorption isotherm applied to occupancy of the kink sites. Finally, we investigate the response of the system when a completely blocking electrode is attached, with the physical separation between the equipotential plane of the electrode and the plane of the electrical centers of the "adsorbed" surface charges explicitly introduced. Free energy minimization in this situation leads to Langmuir adsorption at the surface. A new equivalent circuit representing the total differential capacitance of the system is derived, and competing effects of adsorption capacitance, diffuse double layer capacitance, and separation capacitances are investigated. An important result is that we find the surface adsorption capacitance to be essentially in parallel rather than in series with the diffuse double layer capacitance. Numerous analytic and numerical results of capacitance versus temperature and applied bias are presented for different limiting surface site concentrations and it is found that the surface potential plays somewhat the role of a diffusion potential, causing the minimum of the diffuse layer capacitance (occurring at the "flat-band potential") and the maximum of the adsorption capacitance to be displaced from one another in potential. Some of the results of the present work also may be relevant to the theory of adsorption capacitance in unsupported aqueous electrolytes.

I. INTRODUCTION

The equilibrium distribution of space charge near the surface of an ionic crystal has been the subject of numerous theoretical and experimental studies.[1-8] To set the stage for the present work we will briefly review a number of these contributions, with emphasis upon the physical situations considered and the approximations and assumptions made in each case.

For the moment we restrict our consideration to binary crystals of chemical formula AB, and let N denote the concentration of anion or cation sites. [A glossary of symbol definitions appears at the end of this paper.] For simplicity we assume the bulk of the crystal to be stoichiometric and the lattice disorder to be exclusively of either the Schottky or Frenkel-type. We let c_0 denote the bulk concentration of positive and negative ion vacancies (Schottky disorder) or positive ion interstitials and positive ion vacancies (Frenkel disorder) and define the bulk fractional defect concentration δ as c_0/N. This important parameter appears in the entropy contribution to the free energy of the crystal when account is taken of the lattice structure (lattice gas statistics) and reflects some of the consequences of finite ion size. Neglecting the charge carrier concentration in comparison with N amounts to the assumption of ideal gas statistics for the charge carriers.

In Refs. 1, 3–5, 7, and 8, the assumption that the charge carrier concentrations are everywhere small compared to N has been made either implicitly[1,5,7,8] or explicitly[3,4] before the electric field dependence on local potential is calculated. This approximation has the actual effect of eliminating the lattice gas restriction on the magnitudes of the charge carrier concentrations, leaving them free to increase without limit. An important part of the present study is the analysis of situations in which δ is not negligible compared to unity (the usual case in superionic conductors, such as β-alumina) and those in which the concentration of charge carriers in the interfacial region is significant compared to N, even though δ itself may be quite small. In such situations, finite ion (or vacancy) size should not be neglected. It will be dealt with in the present work by the adoption of an explicit lattice gas model.[9]

 0021-9606/80/225272-22$01.00

References 2 and 3 treat crystals of finite size (two surfaces of interest in the usual one-dimensional approximation) while the rest involve the assumption of a semi-infinite crystal with no perturbation present far away from the single surface of interest. Further, Refs. 1–3, 6, and 8 assume Schottky disorder and 4, 5, and 7 consider Frenkel disorder. Only Refs. 5 and 7 consider the possibility of a limiting concentration, Γ_s per unit area, of surface sites (termed N_s in these references) possibly much smaller than the corresponding concentration of ion sites in an interior lattice plane parallel to the electrode. Other treatments have less realistically set no limits on surface site occupancy, or when an electrode is present, taken surface charge to be identically zero. References 5 and 7 assume that the only surface sites energetically available to the mobile charges are kink sites. Then for an uncharged surface of a Frenkel defect conductor, one-half of the kink sites ($\Gamma_s/2$ per unit area) will be occupied by metal ions and the remaining half by negative ions.[5,7] References 3–5, and 7 have dealt with no-electrode situations and 1, 6, and 8 have assumed completely blocking electrodes. Only Refs. 6 and 8 have considered to some extent the differential capacitance of electrode/crystal systems.

Grimley was the first worker to analyze the arbitrary δ situation.[2] He examined the contact between an electrolyte solution and a single crystal having Schottky disorder. By free energy minimization he obtained solutions for field and charge distributions vs local potential in both phases for both finite and semi-infinite crystals. His results, which take some account of the lattice nature of the solid, are very similar for the two phases. Although the boundary conditions used by Grimley[2] and by Kliewer and Koehler[3] are somewhat different, Grimley's results for the field and charge concentrations in the surface region of the crystal are exactly the same as those which Kliewer and Koehler would have found in both the finite and semi-infinite cases, had they not taken δ to be negligible.

Let us use L_D to denote the Debye length in the bulk of a crystal of length l. In the situation where $l/L_D \gg 1$, one may consider a single surface of the crystal, assuming bulk conditions to hold in the crystal interior and thus deal with a semi-infinite case. The solution for effective potential vs position measured from the surface obtained by Kliewer and Koehler[3] in this case, with δ negligible, is of the same form, when one uses the identity $\tanh(z_0/4) \equiv \mathrm{sgn}(z_0)\exp[-\sinh^{-1}\{\mathrm{csch}(z_0/2)\}]$, as that found much earlier by Macdonald and Brachman,[10] itself a form of the Gouy diffuse double layer solution given long ago.[11]

In the present work, we shall show how three different approaches can lead to the same charge distributions in the arbitrary δ situation, thus providing some additional physical insight into this case. In addition, we shall explore predictions obtained from the general solution when Γ_s is not taken infinite in both the semi-infinite and finite length situations. In the latter case, we shall, however, assume that $l/L_D \gtrsim 20$, so that conditions at the two surfaces are uncoupled except through the unequal division of any applied potential difference between the two regions. We shall devote especial attention to differential capacitance behavior since this may prove a valuable diagnostic tool, possibly better in some ways than the vibrating capacitor technique used by Danyluk and Blakely.[12] Although the present work, like all its predecessors in this field, takes no account of the attractive and repulsive interactions between neighboring charges except through the coarse-grained electric field obtained on integration of the Poisson equation, we plan in future work to show how some of these interactions may be introduced in a lattice gas model for charged crystal defects. In Sec. II we shall consider only electrode or surface charge situations, reserving analysis and discussion of the more general situation where both may be simultaneously present for Sec. III. Further, to maintain continuity with past work in this field, we shall ignore certain aspects of ion size in the interphase region in II but not in III.

II. INITIAL ANALYSIS

A. Current and charge distribution equations

In this section we demonstrate how results for the arbitrary δ situation for Schottky or Frenkel disorder can be obtained by different methods from overtly different assumptions for the case of limited or unlimited Γ_s. Further, the quasithermodynamic approach to be described is also applicable in nonequilibrium situations.[13]

Let $i = 1, 2$, with c_i the volume concentration of the ith species of charge carrier of valence number z_i ($z_i \geq 1$). For generality we allow $z_1 \neq z_2$ in the Schottky case; $z_1 = z_2$ is required for materials with Frenkel defects in only one sublattice. We shall make the identifications $c_1 \equiv n$ and $c_2 \equiv p$, where n and p denote concentrations of negative and positive charge carriers (ions and vacancies in the Frenkel case). The chemical and electrochemical potentials of species i are defined in the usual way as

$$\mu_i = \mu_i^0 + kT \ln(a_i) \tag{1}$$

and

$$\eta_i = \mu_i + (-1)^i z_i e\psi \ , \tag{2}$$

where μ_i^0 is the standard state chemical potential, a_i is the activity of species i, e is the proton charge, and ψ is the local potential, related to the local mean field by $\partial\psi/\partial x = -E$. The Faradaic current associated with species i may be obtained from

$$I_i = (-1)^i e z_i c_i (D_i/kT)\left(-\frac{\partial \eta_i}{\partial x}\right) \ , \tag{3}$$

for the one-dimensional current flow situation considered here.[14] Using the Einstein relation between diffusion coefficients and mobilities, $D_i = (kT/e)(\mu_{mi}/z_i)$ where μ_{mi} is the mobility of the ith species, one finds that Eqs. (1)–(3) lead to

$$I_i = (-1)^i e z_i \left[(-1)^i \mu_{mi} c_i E - D_i (c_i/a_i)\left(\frac{\partial a_i}{\partial x}\right)\right] \ , \tag{4}$$

which reduces to the ordinary dilute-concentration form of the Nernst–Planck equation as $c_i \to 0$ and $a_i \to c_i$.

Finally, on defining the thermodynamic factor $T_i \equiv (c_i/a_i)(\partial a_i/\partial c_i)$, one has

$$I_i = (-1)^i e z_i \mu_{mi} \left[(-1)^i c_i E - \left(\frac{kT}{ez_i} \right) T_i \frac{\partial c_i}{\partial x} \right] , \quad (5)$$

where $T_i \to 1$ in the dilute limit. In time-dependent situations the total current density is given by $I = I_1 + I_2 + I_d$, where I_d is the displacement current contribution.[14] We shall solve Eq. (5) for the equilibrium case shortly.

We adopt a "noninteracting" lattice gas model, in which one has[9] $a_i = c_i/[1 - (c_i/N_i)]$ and thus

$$T_i = [1 - (c_i/N_i)]^{-1} . \quad (6)$$

The only interaction between particles in this model arises from their finite size associated in a crystal lattice with N_i, the concentration of lattice sites associated with charge-carrier species i. Thus, for an ionic crystal of NaCl structure with Schottky disorder, $N_i = N$, the concentration of anion or cation sites. For such a material as AgCl which exhibits Frenkel disorder, $N_1 = N$ and $N_2 = 2N$, the concentration of interstitial sites available for the metal ions. We shall refer to these two conditions as the "typical" Schottky case and the "typical" Frenkel case, respectively, and will subsume them into one equation by defining a "structure" factor s_i, with $s_1 = 1$ always and $s_2 = 1$ for the former case and $s_1 = 2$ for the latter. We may then rewrite Eq. (6) as

$$T_i = [1 - (c_i/s_i N)]^{-1} . \quad (6')$$

The less common case of an $A_n B_n$ material may be dealt with by taking $N_1 = N$ as the concentration of cation sites and $N_2 = s_2 N$, the concentration of anion sites with $s_2 = n/m$.

The above forms of a_i and T_i are derived from the partition function for a noninteracting lattice gas.[9] On inserting them in the transport equations one obtains for the equilibrium state, the same results as were obtained in Refs. 2–5 and 7 from directly considering the free energy of the whole crystal. We shall demonstrate this in greater detail later. We have discussed the transport equation approach here because it is directly extendable to the usual nonequilibrium situation in which the departure from equilibrium conditions is small enough to justify the postulate of local equilibrium as employed in nonequilibrium thermodynamics.[15] We shall solve several direct-current situations using these transport equations in future work.

We now present the solution of Eq. (5) for equilibrum conditions. We assume either the absence of an electrode (but an arbitrary surface charge) or a blocking electrode and no surface charge and thus take $I_i = 0$. We can then combine Eqs. (5) and (6′), write $E = -\partial\psi/\partial x$, and solve for ψ as a function of c_i by integration. For a semi-infinite crystal with its surface at $x = 0$, the appropriate boundary conditions are $\psi \to 0$ and $c_i \to c_{i0}$ as $x \to \infty$. Electroneutrality in the bulk requires $z_1 c_{10} = z_2 c_{20}$. As usual, we let c_0 be the common bulk value of c_{10} and c_{20} when $z_1 = z_2$. The semi-infinite case may be approximated in practice by a finite crystal with $l/L_D > 20$ and an ohmic electrode at the right end.

Let us now introduce the normalized local potential $\phi \equiv \psi/(kT/e)$. Then one finds

$$(-1)^i z_i \phi = \ln[(c_{i0}/c_i)\{1 - (c_i/s_i N)\}/\{1 - (c_{i0}/s_i N)\}] . \quad (7)$$

Let $C_i \equiv c_i/s_i N$ and $C_{i0} \equiv c_{i0}/s_i N$ and solve for C_i. Then

$$C_i = [1 + (C_{i0}^{-1} - 1)\exp\{(-1)^i z_i \phi\}]^{-1} = \frac{C_{i0}\exp[(-1)^{i+1} z_i \phi]}{1 + C_{i0}\{\exp[(-1)^{i+1} z_i \phi] - 1\}} . \quad (8)$$

Note that when $z_1 = z_2$, $C_{i0} = \delta/s_i$. In the dilute limit where $C_{i0} \ll 1$, $c_i \to c_{i0}\exp[(-1)^{i+1} z_i \phi]$ the usual Boltzmann distribution. With the earlier definition of s_i, Eq. (8) holds for both Schottky and Frenkel disorder. Its deviation from the Boltzmann form arises entirely because N is limited and indirectly because the charge carriers are of finite size. Nevertheless, Eq. (8) represents a continuum and not a discrete result.

We shall now compare Eq. (8) with results obtained in two other ways. The first such alternative is based on the Langumir isotherm for surface adsorption[16] which is itself based on a two-dimensional lattice gas model.[17] This isotherm assumes a maximum surface occupation density Γ_s and the possibility of only single occupancy of any surface site. Let us begin by conceptually applying this isotherm to each lattice plane parallel to the surface in a single crystal and then carry out the transition from discreteness to the continuum limit for the inner planes, replacing Γ_s by $s_i N$. The general form of an adsorption isotherm is[16]

$$a_B \exp[-\Delta\bar{G}_i^0/kT] = a_i \quad (9)$$

where a_B is the unperturbed bulk activity, a_i the activity of the adsorbed species, and $\Delta\bar{G}_i^0$ is the standard free energy difference between the bulk and the adsorption plane.

In accord with the general outline given above, we take the Langmuir form of the isotherm using the lattice gas expression for a_i with $N_i \equiv s_i N$. The same result is appropriate for a_B with c_i replaced by c_{i0}. For the present case $\Delta\bar{G}_i^0$, the standard free energy of adsorption (site occupancy) is potential-dependent. Introducing this dependence in the conventional way,[9,18] we write $\Delta\bar{G}_i^0 = (-1)^i e z_i \psi$. Equation (9) then becomes

$$c_i/[1 - (c_i/s_i N)] = [c_{i0}/\{1 - (c_{i0}/s_i N)\}]\exp[(-1)^{i+1} z_i \phi] , \quad (10)$$

a relation entirely equivalent to Eq. (8).

The Langmuir isotherm, when applied to the interior region of the crystal is thus thermodynamically equivalent to the lattice gas model under equilibrium conditions. This observation which follows from the particularly simple form of the partition function for the lattice gas in two or three-dimensions can serve as the starting point for several different lines of investigation. For example, various modifications,[16] mostly somewhat heuristic, have been made to the ordinary Langmuir isotherm to account for attractive and re-

pulsive interactions between adsorbed species that go beyond the hard sphere model implict in the Langmuir isotherm itself. These same modifications when transformed as above for a volume rather than surface charge distribution may be useful in guiding the choice of the form of activity expressions to take such interactions into account and can be used in the transport equation (5) in both equilibrium and nonequilibrum situations.

Finally, it is of interest to compare the present results for C_i with $z_1 = z_2 = 1$ with those obtained by Poeppel and Blakely before δ was implicitly set to zero in their work.[5] Theirs is a semi-infinite free surface situation and they take the zero of potential at the surface of interest. With our zero in the bulk, their ϕ_∞ equals $-\psi_s \equiv -(kT/e)\phi_s$, where ϕ_s is the present normalized surface potential in the absence of any applied potential. When the Poeppel–Blakely Eq. (I-5) is expressed in the present notation, one obtains

$$\frac{C_i}{1-C_i} = \left(\frac{\Gamma_s + 2(-1)^i(\sigma_s/e)}{\Gamma_s - 2(-1)^i(\sigma_s/e)}\right)\exp[-\mathcal{G}_i + (-1)^{i+1}(\phi - \phi_s)] , \tag{11}$$

with $\phi = \phi_s$ at the surface and $\phi = 0$ in the bulk. Here Γ_s is the number of surface sites per unit area (taken as kink sites[5]); σ_s is the net surface charge per unit area, given here by[5] $\sigma_s = e[\Gamma_2 - (\Gamma_s/2)]$ where Γ_2 is the number of positive ions in surface sites per unit area; $\mathcal{G}_i \equiv \Delta G_i/kT$, and the present ΔG_i's are the free energies of formation of the charged species, here vacancies and interstitials. In this typical Frenkel case, $s_1 = 1$ and $s_2 = 2$. When $\phi = 0$, $C_i = \delta/s_i$ and Eq. (11) yields in this limit

$$\frac{\delta}{1-\delta} = \left(\frac{1-2\omega}{1+2\omega}\right)\exp(-\mathcal{G}_1 - \phi_s) \tag{12}$$

and

$$\frac{(\delta/2)}{1-(\delta/2)} = \left(\frac{1+2\omega}{1-2\omega}\right)\exp(-\mathcal{G}_2 + \phi_s) , \tag{13}$$

where $\omega \equiv (\sigma_s/e\Gamma_s) \equiv (\Gamma_2/\Gamma_s) - 0.5$ and 2ω thus represents the relative deviation of Γ_2 from its surface-neutral value of $\Gamma_s/2$. Necessarily $-0.5 \leq \omega \leq 0.5$, although the limits are never attained at finite temperature. The product of Eqs. (12) and (13) is

$$\frac{(\delta^2/2)}{(1-\delta)[1-(\delta/2)]} = \exp(-\mathcal{G}_+) , \tag{14}$$

where $\mathcal{G}_+ \equiv \mathcal{G}_1 + \mathcal{G}_2$. This is a form of mass action law since the left-hand side of Eq. (14) is N^{-2} times the product of the bulk activities of the mobile charges in the lattice gas model; it may be solved for δ as a function of $\mathcal{G}_+$. The maximum value of δ is, of course, unity, and for $\mathcal{G}_+ \gg 1$, $\delta \cong \sqrt{2}\exp(-\mathcal{G}_+/2) \ll 1$. By taking the quotient of Eqs. (13) and (12), one obtains

$$\begin{aligned}\phi_s &= 0.5\,[\ln\{\{(1-\delta)/(2-\delta)\}\{(1-2\omega)/(1+2\omega)\}^2\} - \mathcal{G}_-] \\ &\equiv \phi_{s0} - 2\tanh^{-1}(2\omega) \\ &\equiv \phi_{s0} - 2\tanh^{-1}(\sigma_s/\sigma_{sm}) ,\end{aligned} \tag{15}$$

where

$$\phi_{s0} \equiv 0.5\,[\ln\{(1-\delta)/(2-\delta)\} - \mathcal{G}_-] . \tag{16}$$

Here $\mathcal{G}_- \equiv \mathcal{G}_1 - \mathcal{G}_2$, $\sigma_{sm} \equiv e\Gamma_s/2$, the maximum surface charge, and ϕ_{s0} is the value of ϕ_s at the point of surface neutrality, $\omega = 0$. Equation (15) sets a simple but crucially important relation between the normalized surface charge and the potential in the plane of this charge ϕ_s. It specifies that because of the thermodynamic requirements of the situation, it would be necessary to establish a p.d. of ϕ_{s0} between the plane of the charge and the bulk in order to force σ_s to be zero. The above result for ϕ_s is expressed in its most transparent form here but is entirely equivalent to the Poeppel and Blakely result for ϕ_∞ $(= -(kT/e)\phi_s)$. We may now use Eqs. (12) and (13) to eliminate $\mathcal{G}_i$ and ϕ_s from Eq. (11), yielding

$$\frac{C_i}{1-C_i} = \left[\frac{(\delta/s_i)}{1-(\delta/s_i)}\right]\exp[(-1)^{i+1}\phi] , \tag{11'}$$

which is again entirely equivalent to Eq. (8) in the $z_1 = z_2 = 1$ case appropriate for a free AgCl surface as considered by Poeppel and Blakely.

We have now seen that the same distribution function $C_i(\phi)$ for the arbitrary δ case may be obtained in three different but interrelated ways. We next make use of these distributions to obtain the differential capacitance when Γ_s and δ are both arbitrary. Although we shall be particularly concerned in this paper with AgCl and similar materials, it has been suggested[19] that a lattice gas model such as that we are considering here is especially appropriate for the superionic conductor α-AgI.

B. Field expressions

Poisson's equation may be written in the intrinsic and time-independent case as

$$\frac{dE}{dx} = (4\pi e/\epsilon_B)(z_2 c_2 - z_1 c_1) , \tag{17}$$

where ϵ_B is the bulk low frequency dielectric constant. We normalize E and x so that $\mathcal{E} \equiv E/(kT/eL_D)$ and $X \equiv x/L_D$, where

$$\begin{aligned}L_D &\equiv [\epsilon_B\, kT/4\pi e^2(z_1^2 c_{10} + z_2^2 c_{20})]^{1/2} \\ &\equiv [2/z_1(c_{10}/N)(z_1+z_2)]^{1/2} L_{DN}\end{aligned} \tag{18}$$

with

$$L_{DN} \equiv [\epsilon_B\, kT/8\pi e^2 N]^{1/2} . \tag{19}$$

Here use has been made of the relation $z_1^2 c_{10} + z_2^2 c_{20} = z_1 c_{10}(z_1 + z_2)$. Equation (17) may now be written in normalized form as

$$\begin{aligned}\frac{d\mathcal{E}}{dX} &= \frac{z_2 s_2 C_2 - z_1 s_1 C_1}{z_1(c_{10}/N)(z_1+z_2)} \\ &\equiv J(\phi) ,\end{aligned} \tag{17'}$$

where the C_i's are given by Eq. (8). Now since $\mathcal{E} = -d\phi/dX$, $d\mathcal{E}/dX = -\mathcal{E}\,d\mathcal{E}/d\phi$. Therefore, for the semi-infinite case, we may write the general expression

$$2\int_0^{\mathcal{E}} \mathcal{E}'\,d\mathcal{E}' = \mathcal{E}^2 = -2\int_0^{\phi} J(\phi')\,d\phi' , \tag{20}$$

leading to

$$\begin{aligned}\mathcal{E}^2 = [2N/(z_1+z_2)z_1 c_{10}]\ln[\{1 + C_{10}[\exp(z_1\phi) - 1]\}^{s_1} \\ \times\{1 + C_{20}[\exp(-z_2\phi) - 1]\}^{s_2}] .\end{aligned} \tag{21}$$

From now on we consider only the usual $z_1 = z_2 = 1$ case. Then for typical Schottky disorder, Eq. (21) yields

$$\mathcal{E}^2 = \delta^{-1} \ln(1 + R_1) , \tag{22}$$

where

$$R_1 \equiv 4\delta(1 - \delta) \sinh^2(\phi/2) . \tag{23}$$

In the $\delta \to 0$ limit, one obtains the usual result

$$\mathcal{E} = 2 \sinh(\phi/2) . \tag{24}$$

Matters are somewhat more complicated for typical Frenkel disorder. Then

$$\mathcal{E}^2 = \delta^{-1} \ln[\{1 + \delta[\exp(\phi) - 1]\}\{1 + (\delta/2)[\exp(-\phi) - 1]\}^2] \tag{25}$$

which after considerable algebra reduces to

$$\mathcal{E}^2 = \delta^{-1} \ln(1 + R_2) , \tag{25'}$$

where

$$R_2 \equiv A_2 - B_2 , \tag{26}$$

and

$$A_2 = 4\delta \sinh^2(\phi/2) \tag{27}$$

and

$$B_2 = [\delta \sinh(\phi/2)]^2 \{3 + (1 - \delta)[1 - \exp(-\phi)]\} . \tag{28}$$

In contrast to the typical Schottky case, the present $\mathcal{E}^2$ is unsymmetrical in $\pm\phi$ unless $\delta \to 0$. In this limit Eq. (24) is again obtained.

We shall next explore several specific semi-infinite crystal situations for arbitrary δ going from simple to more complicated. First, we consider the situation in which no surface charge σ_s exists but a metallic electrode is present. Next follows further analysis of the Poeppel–Blakely situation, in which no electrode is present but a definite surface charge layer exists at $x = 0$ so that $\sigma_s \neq 0$. Finally we shall consider the case in which both a surface charge layer and a metallic electrode are present simultaneously. If we denote the charge density on the electrode by σ_m and the diffuse double layer space charge integrated from $x = 0$ to $x = \infty$ by σ_d, then overall charge neutrality requires that

$$\sigma_m + \sigma_s + \sigma_d = 0 \tag{29}$$

in this latter case. Here all quantities are charge per unit area.

C. Blocking electrode, no surface charge

Since the electrode is assumed to be completely blocking, I_1 in Eq. (5) is zero and as we have seen we obtain the C_i's of Eq. (8) and thus the $\mathcal{E}^2$'s of Eq. (22) for the typical Schottky case and Eq. (25') for the typical Frenkel case. Now we explicitly take $\sigma_s = 0$, so $\sigma_m = -\sigma_d$. Gauss' law immediately leads to

$$\sigma_m = (\epsilon_B/4\pi) E_m = (\epsilon_B/4\pi L_D)(kT/e) \mathcal{E}_m \equiv C_d V_T \mathcal{E}_m = C_0 V_T \sqrt{\delta}\, \mathcal{E}_m , \tag{30}$$

where $\mathcal{E}_m$ is the field at the surface of the electrode. Here $C_d \equiv \epsilon_B/4\pi L_D$ is the usual diffuse double layer capacitance per unit area in the limit of zero p.d. All appropriate quantities will be specified per unit area from this point on. The capacitance $C_0 \equiv (L_D/L_{DN}) C_d = C_d/\sqrt{\delta}$ is independent of δ and $V_T \equiv kT/e$ is the thermal voltage.

We assume that the charge on the electrode is produced by an effective potential, $\psi_e \equiv \psi_a + \psi_D$, where ψ_a is the applied potential difference and ψ_D is an additional potential difference which takes into account the potential of the reference electrode and allows for the possibility that charge transfer may have occurred between the blocking electrode and the crystal during preparation of the interface, even though the interface, once prepared, is taken completely blocking to all charges. Some additional discussion of ψ_D is given in Ref. 8. ψ_D will be taken independent of ψ_a for simplicity here. On normalizing all charges per unit area with $\sigma_n \equiv C_d V_T$ so that $Q_m \equiv \sigma_m/\sigma_n$, etc., we obtain in the present situation $Q_m = \mathcal{E}_m = -Q_d$, and $\mathcal{E}_m$ is given by Eq. (22) or (25') with ϕ replaced by $\phi_e \equiv (\phi_a + \phi_D)$.

We may define a normalized static or integral capacitance by $C_{SN} \equiv C_S/C_d \equiv Q_m/\phi_a = \mathcal{E}_m/\phi_a$ and a normalized differential capacitance by

$$C_{DN} \equiv C_D/C_d \equiv dQ_m/d\phi_a = d\mathcal{E}_m/d\phi_a . \tag{31}$$

Since C_{DN} is the quantity of usual experimental interest, we shall consider it only from now on. Let $M_i \equiv \ln(1 + R_i)$ and $Z_i \equiv dR_i/d\phi_a$. The R_i's are here given by Eqs. (23) and (26) with ϕ replaced by $\phi_a + \phi_D$. For both Schottky and Frenkel disorder $\mathcal{E}_m = [\delta^{-1} M_i]^{1/2}$. Thus

$$C_{DN} = Z_i/2(1 + R_i)(\delta M_i)^{1/2} . \tag{32}$$

For Schottky disorder, one finds

$$Z_1 = 2\delta(1 - \delta) \sinh(\phi_a + \phi_D) , \tag{33}$$

while in the Frenkel case,

$$Z_2 = 2\delta[1 - (B_2/A_2)] \sinh(\phi_a + \phi_D) + B_2 - A_2\delta[1 - (\delta/4)] , \tag{34}$$

where A_2 and B_2 are given in Eqs. (27) and (28) with ϕ replaced by $(\phi_a + \phi_D)$. A relatively simple expression results for C_{DN} in the Schottky case. It is

$$C_{DN} = \frac{\delta(1 - \delta) \sinh(\phi_a + \phi_D)}{[1 + 4\delta(1 - \delta) \sinh^2\{(\phi_a + \phi_D)/2\}] \cdot [\delta \ln\{1 + 4\delta(1 - \delta) \sinh^2\{(\phi_a + \phi_D)/2\}\}]^{1/2}} . \tag{35}$$

As $\delta \to 0$, this reduces to the well-known result[8]

$$C_{DN} = \cosh[(\phi_a + \phi_D)/2] , \tag{36}$$

which strictly applies for arbitrary ϕ_e only when $\delta = 0$. When $R_1 = 4\delta(1 - \delta)\sinh^2[(\phi_a + \phi_D)/2] \gg 1$, Eq. (35) leads to

$$C_{DN} \cong [4\delta\{|\phi_a + \phi_D| + \ln\{\delta(1 - \delta)\}\}]^{-1/2} . \tag{37}$$

The expression for $\mathcal{E}_m$ obtained above for typical Schottky disorder is equivalent when ϕ_D is set to zero

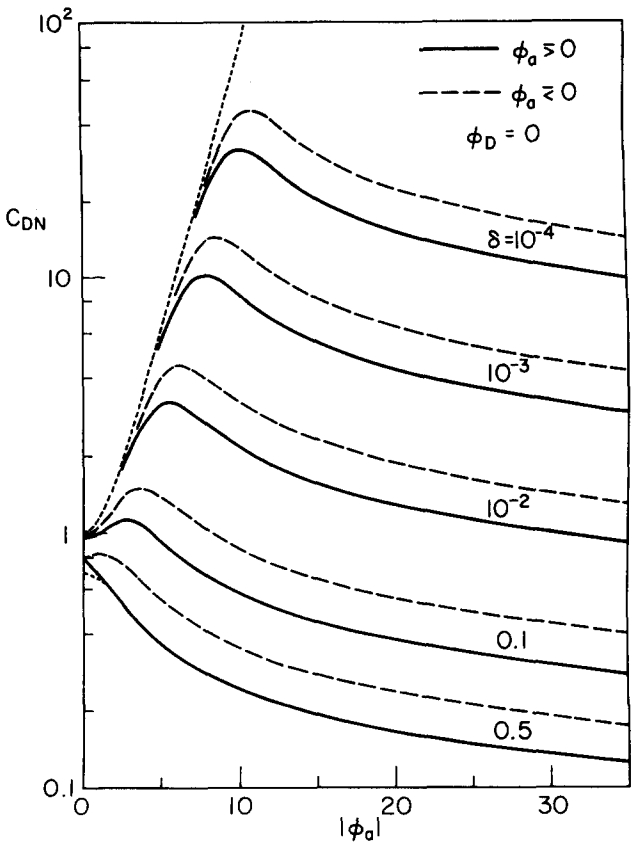

FIG. 1. Normalized total differential capacitance C_{DN} vs normalized applied p.d. ϕ_a for various δ values. Results apply for a single blocking electrode, Frenkel defect situation.

to that obtained originally by Grimley.[2] Grimley's result has been used by Raleigh[6] to obtain an expression for C_D consistent with that of Eq. (35) and a limiting form consistent with (37) when δ is neglected compared to unity. Note that (37) yields $C_{DN} \propto \psi_e^{-1/2}$ for $|\phi_e| \gg |\ln\{\delta(1-\delta)\}|$. This is a familiar relation in semiconductor physics where it is associated with the formation of a charge carrier depletion region near a junction or electrode.[20] Here, however, it is associated with the formation of an accumulation region of a special kind, one where a region of nearly constant charge density builds up from the electrode out into the material. In contrast to the conventional picture of an accumulation layer of point charges, in which the charge density near the electrode may increase without limit, here c_1 and c_2 can never exceed N.

In the $\delta \to 0$ limit, Z_1 and Z_2, R_1 and R_2, and M_1 and M_2 all approach each other, and Eq. (36) for C_{DN} applies for either type of disorder. Alternatively, in the $\phi_e \to 0$ limit, C_{DN} approaches $(1-\delta)^{1/2}$ for Schottky disorder and $[1-(3\delta/4)]^{1/2}$ for Frenkel disorder.

For $\phi_D = 0$, curves of C_{DN} vs $|\phi_e| = |\phi_a|$ are shown in Fig. 1 with δ a parameter. The top dotted curve is that for $\delta \to 0$; the bottom one is for typical Schottky disorder; all other curves are for the typical Frenkel situation. The dashed and solid curves show the asymmetry in Frenkel results for $\phi_e > 0$ and $\phi_e < 0$. They differ for sufficiently large $|\phi_e|$ by very nearly a factor of $\sqrt{2}$, the difference ultimately arising from the $s_1 = 1$, $s_2 = 2$ values appropriate in this case. Surprisingly the Schottky results (symmetrical in ϕ_e) are found to agree with the $\phi_e \geq 0$ Frenkel ones too closely for graphical separation except for the bottom dotted curve in the region $0 \leq \phi_e < 2$. A single Schottky curve (for $\delta \ll 1$) like those of Fig. 1 has been calculated by Raleigh[6] and employed in the interpretation of capacitance data for AgBr, a typical Frenkel defect material. As we have seen above, for one of the two possible polarities of the interfacial potential (here ψ_a), there is no measurable distinction between Schottky and Frenkel C_D results for $\delta \leq 0.1$. For $\phi_D \neq 0$, the curves of Fig. 1 still apply if the $|\phi_a|$ scale is replaced by $|\phi_e|$ so that $\phi_e = 0$ corresponds to $\phi_a = -\phi_D$.

Let us next consider completely blocking two-electrode situations (finite separation length l) chosen so that $L \equiv l/L_D$ is $\gtrsim 20$, resulting in negligible overlap of the volume space charge distributions associated with each electrode for a substantial range of applied potential differences. For maximum generality we associate a fixed reference potential ψ_{DL} with the left electrode/material interface and a fixed, possibly different reference potential ψ_{DR} (allowing for different electrode materials) with the right interface. The applied p.d. ψ_a is divided between the two space charge regions so that $\psi_a = \psi_{aL} + \psi_{aR}$ and the effective potential across the left region is $\psi_{eL} = \psi_{DL} + \psi_{aL}$ and that across the right is $\psi_{eR} = \psi_{DR} + \psi_{aR}$. With the present choice of signs if $\psi_a > 0$, then both ψ_{aL} and ψ_{aR} will be positive.

In general, the effective potential does not divide equally between the two regions even when $\psi_{DL} = \psi_{DR}$. Because of the $L \gg 1$ assumption introduced above, we may apply the semi-infinite case results just discussed to each region provided that ψ_{eL} and ψ_{eR} are properly determined. They must be consistent with the condition $\sigma_m(\psi_{eL}) + \sigma_m(\psi_{eR}) = \sigma_m(\psi_{DL}) + \sigma_m(\psi_{DR})$ which follows from overall charge neutrality and the assumed complete blocking of charge transfer between the electrodes and the crystal. On transforming to normalized variables, one may write the equations which determine ϕ_{aL} and ϕ_{aR} as

$$\begin{aligned} \phi_a &= \phi_{aL} + \phi_{aR} , \\ \phi_{eL} &= \phi_{DL} + \phi_{aL} , \\ \phi_{eR} &= \phi_{DR} + \phi_{aR} , \end{aligned} \tag{38}$$

and

$$Q_m(\phi_{eL}) + Q_m(\phi_{eR}) - Q_m(\phi_{DL}) - Q_m(\phi_{DR}) \equiv \mathcal{E}_m(\phi_{eL}) + \mathcal{E}_m(\phi_{eR}) - \mathcal{E}_m(\phi_{DL}) - \mathcal{E}_m(\phi_{DR}) = 0 . \tag{39}$$

Equation (39) must be solved by iteration to obtain say ϕ_{aL}, given ϕ_a, ϕ_{DL}, and ϕ_{DR}.

Figure 2 shows some results for the typical Frenkel disorder situation with $\phi_{DL} = \phi_{DR} = 4$. We have plotted $C_{DN} = [C_{DNL}^{-1} + C_{DNR}^{-1}]^{-1}$ vs $|\phi_a|$ here since C_{DN} is symmetric in ϕ_a for this $\phi_{DL} = \phi_{DR}$ case. Shown dotted is a curve for $\phi_{DL} = \phi_{DR} = 0$ and $\delta \to 0$. At $\phi_a = 0$, the C_{DN} values for the solid curve are, of course, just half of the corresponding C_{DN} values for the semi-infinite case at $\phi_a = 0$. The dashed $\delta = 0$ C_{DN} curve of Fig. 2 is of the

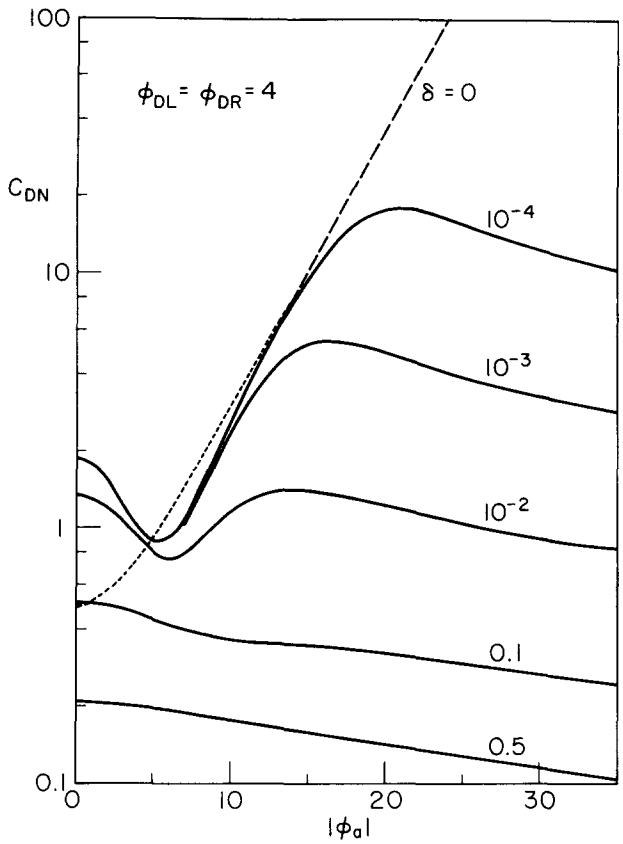

FIG. 2. C_{DN} vs $|\phi_a|$ for a Frenkel defect situation with two blocking electrodes and $\phi_{DL} = \phi_{DR} = 4$.

same form as found earlier[8] when the parameter λ of the earlier work is taken zero. There, normalization was with $0.5\, C_d$, however, instead of the present C_d.

To illustrate some of the complexity of C_{DN} curves possible when $\phi_{DL} \neq \phi_{DR}$, we have presented curves for different δ's with $\phi_{DL} = 12$, $\phi_{DR} = 3$ (dashed) and $\phi_{DL} = 2$, $\phi_{DR} = 6$ (solid) in Fig. 3. Note that these curves are symmetric around the value $\phi_a = \phi_{DR} - \phi_{DL}$, -9 and 3 in the present cases (see arrows). The separation between the minima of the curves is 2 max (ϕ_{DL}, ϕ_{DR}).

D. No electrode, surface charge present

This is the situation analyzed by Poeppel and Blakely[5] (abbreviated hereafter as P–B) in the $\delta \to 0$ limit. Here we shall investigate the consequences of a finite value for δ and consider the capacitance possibilities.

In the present no-electrode situation Gauss' law leads to $\sigma_s \equiv e\Gamma_s \omega = (\epsilon_B/4\pi) E_s = C_0 V_T \sqrt{\delta}\, \mathcal{E}_s$. We define the temperature-dependent quantity $H \equiv C_0 V_T / e\Gamma_s$. Following P–B we shall apply the results of this section to the Frenkel-disorder material AgCl. Then $N \cong 2.336 \times 10^{22}$ cm^{-3} and $H \cong 1.607 \times 10^{14} (\epsilon_B kT)^{1/2}/\Gamma_s$. In order to take the dependence of ϵ_B on T into account, we use an expression for $\epsilon_B(T)$ given by Corish and Jacobs.[21] It yields about 12.5 at 200 K and 19.5 at 667 K.

In normalized terms, the above equation for σ_s becomes

$$\omega \equiv H\sqrt{\delta}\, \mathcal{E}_s \equiv H\sqrt{M_2} \equiv H[\ln(1+R_2)]^{1/2}\,, \qquad (40)$$

where R_2 is given by Eq. (26) with ϕ here replaced by the ϕ_s of Eq. (15). Since ϕ_s depends on ω, Eq. (40) is an implicit equation for ω which must be solved by iteration. In the $\delta \to 0$ limit, it is equivalent to the corresponding expression for σ_s given by P–B. We have found it possible to solve this implicit equation accurately for any δ by the Newton–Raphson method, although solution is difficult in nearly saturated regions where $|\omega| \cong 0.5$. A simpler approach will be discussed in the next section.

Since there are no electrodes, one cannot readily apply an external potential to the present system and thus the temperature dependence of various quantities will be of primary interest here. We shall use the same expressions for $\Delta\mathcal{G}_1$ (positive ion vacancy formation energy) and $\Delta\mathcal{G}_2$ (positive ion interstitial formation energy) vs T as have been used previously for AgCl,[3–5,7] although one should recognize that they are not very accurate as the melting temperature is approached.[22] They are, however, quite adequate for illustrative purposes. Then $\mathcal{G}_+ = (1.44/kT) - 9.4$ and $\mathcal{G}_- = (-0.5/kT) - 6.0$.

The ω values obtained from the self-consistent solution of Eq. (40) are found to vary from about 0.004 at 200 K to a maximum of about 0.4993 near 600 K and then decrease slightly to about 0.496 at 10^3 K for $\Gamma_s = 10^{12}$ cm^{-2}. Similar results are found for other Γ_s values. These lead to the curves of Fig. 4 for $\phi_s(T)$ and various Γ_s choices. There is no limitation on surface site density for the $\Gamma_s \to \infty$ curve; steric considerations alone limit Γ_s to a value between 10^{14} and 10^{15} cm^{-2}, however, for AgCl. The dotted line in Fig. 4 indicates the melting point of AgCl. For completeness sake we have extended the temperature scale above the m.p. This may not be wholly unreasonable for silver halides since Raleigh[23] found almost negligible change in the differential capacitance of AgBr on melting.

The curves of Fig. 4 differ only slightly from the corresponding ones for $-\psi_s$ ($\equiv \phi_\infty$ in P–B notation[5]) found by

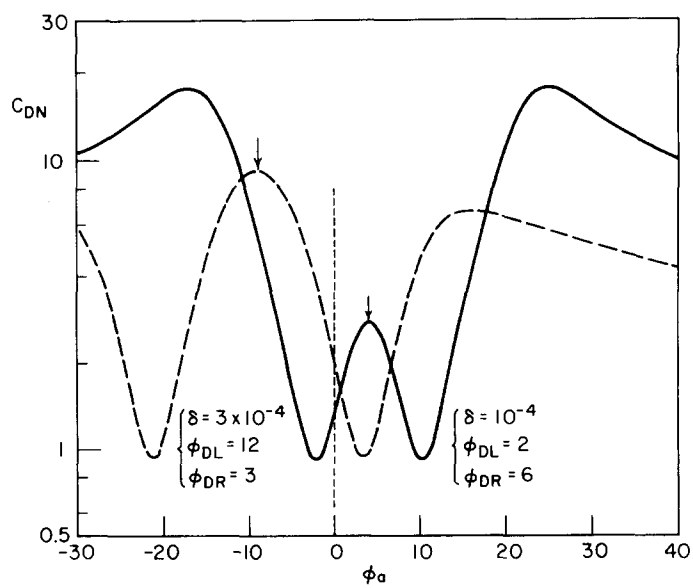

FIG. 3. C_{DN} vs ϕ_a for Frenkel defect situations with $\phi_{DL} \neq \phi_{DR}$ and differing values of δ.

P–B over most of the common temperature range,[5,7] justifying P–B's $\delta \to 0$ approximations. At 200 K, $\delta \simeq 10^{-16}$, yielding a c_0 of only about 2.6×10^{6} cm^{-3}. It increases to 5.6×10^{-4} by 667 K and formally, to 0.0356 at 10^3K. To obtain a precise comparison between ϕ_s calculated with Eq. (40) for arbitrary δ and that essentially equivalent to the corresponding P–B ϕ_s, one merely needs to carry out the $\delta \to 0$ limit for $M_2 \equiv \ln(1+R_2)$ before solving (40). One obtains $M_2 \to R_2 \to A_2 = 4\delta\sinh^2(\phi_s/2)$. By this means we avoid any discrepancies arising from our using a temperature dependent ϵ_B and their presumably taking it constant. For $\Gamma_s = 10^{13}$ cm^{-2}, we find ϕ_s values of 1.1682/1.1677 and 0.09629/0.09496 for $T = 666.\overline{6}$ K and $T = 10^3$ K, respectively. Here the first ϕ_s value was obtained with the arbitrary δ form of Eq. (40) and the second with the small-δ form. For $\Gamma_s = 10^{14}$ cm^{-2}, the corresponding results are 4.6909/4.6698 and 0.9285/0.9083. These are still quite small differences because δ is still appreciably less than unity even at 10^3 K. For some other material (such as Na-β-Al_2O_3) exhibiting higher δ values in the experimental temperature range it would be quite necessary to use the arbitrary-δ results. Although the ϕ_s pairs above are quite close, the value of R_2 was by no means always much smaller than unity. For example, for $\Gamma_s = 10^{14}$ cm^{-2} and $666.\overline{6}$ K, the components of R_2, see Eq. (26), are $A_2 \cong 0.06$ and $B_2 \cong 3.4\times10^{-5}$. For the same Γ_s and 10^3 K, $A_2 \cong 0.033$ and $B_2 \cong 1.1\times10^{-3}$. These results imply that although ϕ_s is relatively insensitive to the small $-\delta$ approximation, some other derived quantities may not be.

In Fig. 5 we show how the surface concentration of interstitials Γ_2 (Ag$^+$ for AgCl) varies with temperature

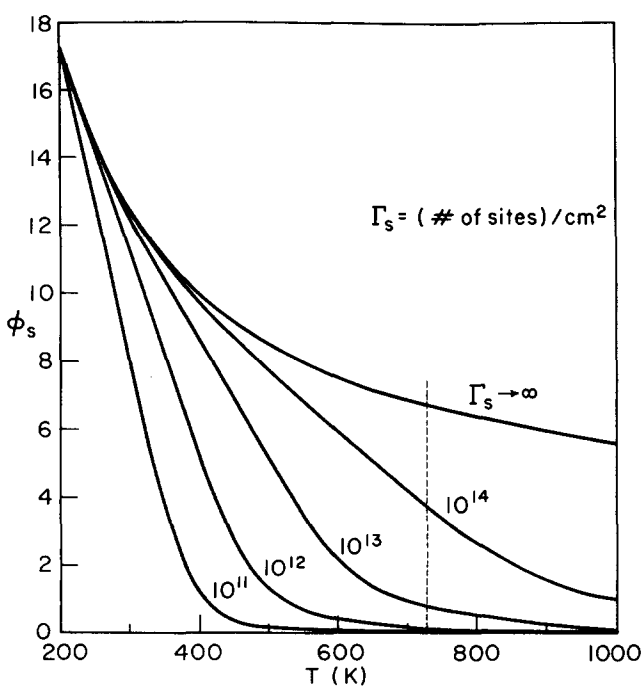

FIG. 4. The normalized surface potential ϕ_s vs temperature for various Γ_s values; no electrode present. Results applicable to AgCl.

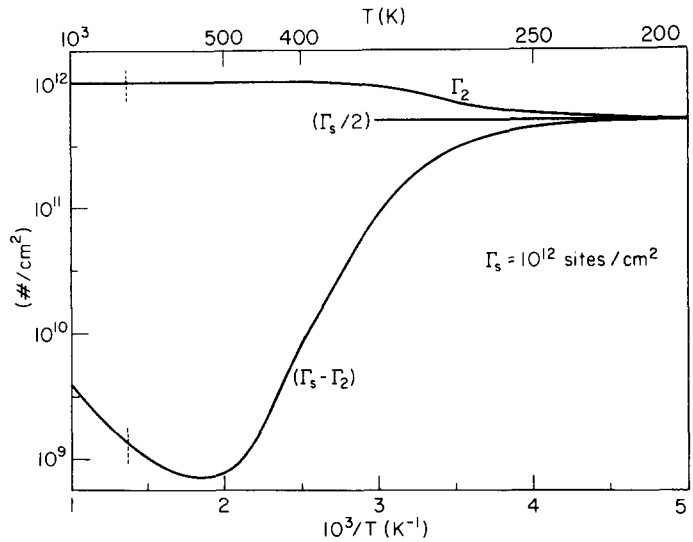

FIG. 5. Dependence of Γ_2 and $(\Gamma_s - \Gamma_2)$ on $10^3/T$ for $\Gamma_s = 10^{12}$ sites/cm^2.

for fixed Γ_s, the total number of interstitial surface sites available equal to 10^{12} cm^{-2}. It is assumed[5] that there are $\Gamma_s/2$ negative kink sites at monomolecular steps (Cl^- for AgCl) that remain fixed and temperature independent. We see that the surface is virtually neutral ($\sigma_s = e[\Gamma_2 - (\Gamma_s/2)] \cong 0$) at low temperature, and that Γ_2 approaches very close to Γ_s near 600 K, then decreases slightly at higher temperatures.

Now analogous to the C_{DN} of Eq. (31) we may define a kind of C_{DN} for the present situation as $C_{DN} \equiv dQ_s/d\phi_s$, where $Q_s \equiv \sigma_s/\sigma_n \equiv \sigma_s/C_d V_T \equiv \mathcal{S}_s = -Q_d$ in the present $Q_m = 0$ case where $\mathcal{S}_s$ is a function only of ϕ_s. The resulting equations for C_{DN} are formally the same as those given in Eqs. (32) through (37) except with ϕ_e replaced everywhere by ϕ_s. But here ϕ_s is not independently variable and for a given system it can only be varied by a temperature change. Therefore it is not very practical to measure the present $C_D \equiv d\sigma_s/d\psi_s$. To do so we might consider applying a small temperature change, resulting in a small change in ψ_s and a change in σ_s. Although the ψ_s change might be measured, at least as a change in relative surface potential by the vibrating capacitor technique,[12] the experimental determination of the change in σ_s and thus in E_s would be very difficult if not impossible. Nevertheless, we have calculated C_D as a function of temperature for the present AgCl situation to show its variation and for comparison with later results obtained for the blocking electrode situation where σ_s and σ_m are both nonzero and dependent on ψ_a.

Results are presented in Fig. 6 for various Γ_s values. Since C_d itself varies with temperature, we have presented C_D rather than C_{DN} and also show the C_d variation. The dashed line at the left shows its deviation from linearity in this semilog vs $10^3/T$ plot. This deviation arises both because of the change of dielectric constant with temperature which we have included and also because the exact quadratic expression for $\delta(T)$, Eq. (14) must be used in the high temperature regime. Figure 6 shows that C_D approaches the C_D for $\Gamma_s \to \infty$ at sufficiently

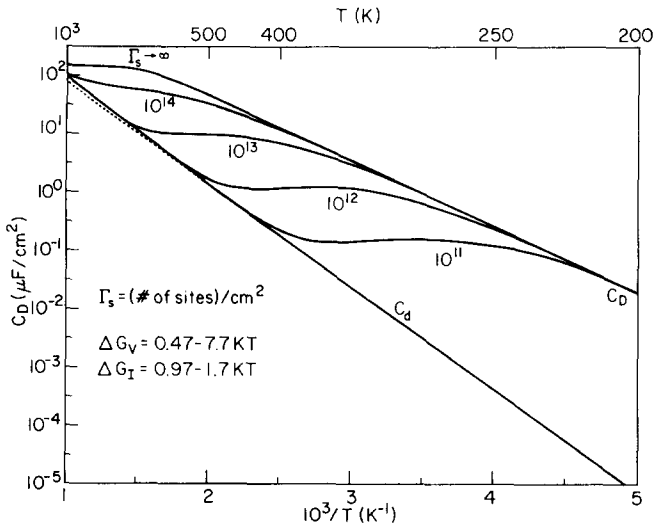

FIG. 6. The synthetic capacitance $C_D = d\sigma_s/d\psi_s$ vs T and $10^3/T$ for various Γ_s values. Also shown is the C_d temperature dependence appropriate for AgCl.

low temperature for any Γ_s and correspondingly approaches C_d (more precisely, $C_d[1-(3\delta/4)^{1/2}]$ at the temperature where ϕ_s is less than unity and becoming negligible. Between these extremes, there are quite wide temperature ranges where C_D remains nearly temperature independent.

The differences between the C_D's calculated with the general formula applicable for any δ and those calculated with the P–B approximation by assuming $R_2 \ll 1$ so that $M_2 \cong R_2$ begin to become significant as T becomes large and as Γ_s increases. For example, corresponding C_D values in μF/cm^2 are 56.58/58.50 and 103.3/107.2 for $\Gamma_s = 10^{14}$ cm^{-2} and $T = 666.\bar{6}$ K and 10^3 K. The accurate results appear first in each pair and the approximate ones second. For $\Gamma_s \to \infty$, results for the same two temperatures are 130.7/186.5 and 154.2/782.9. Although the $T = 10^3$ K comparisons are probably not very meaningful for the specific AgCl case, they nevertheless show how large the differences can become in cases where the $M_2 \cong R_2$ approximation is unjustified.

Thus far we have taken some account of the finite size of ions (and vacancies) by means of the lattice gas model. We have, however, neglected one important consequence of finite ion size with regard to the surface, in that we have followed P–B in assuming zero separation between the surface layer and the underlying material. Because of finite ion size there is actually some separation between the electrical centers of the surface charge and the first interior layer of the crystal and, as well, separation between the effective plane of the surface charges and the effective surface plane of the electrode when one is present. It is clearly inconsistent to adopt a three-dimensional lattice gas model for the interior of the crystal, thus taking into account finite ion size both in the planes parallel to the surface and in the direction perpendicular to the surface, while adopting a two-dimensional lattice gas model for the surface plane and neglecting the finite size of the surface ions when dealing with the perpendicular direction. Therefore, in the next section we present a consistent treatment which we believe is more physically realistic than any of the previous approaches. We include the possibility of an electrode and a surface charge layer simultaneously present and show how the preceding work in this paper can be further generalized to a situation of great utility in electrical response measurements.

III. FURTHER ANALYSIS AND RESULTS

A. System definition

Figure 7 is an idealized sketch of the interfacial region for a completely blocking metal electrode in contact with the surface of a single crystal material such as AgCl. The region between the phases is termed the inner or compact layer and corresponds to the Helmholtz layer in aqueous electrochemistry. A full description of the relevant theory for the aqueous case is given in Refs. 24 and 25. Here ESP is the electrode surface plane (the surface plane of the perfect conductor which best approximates the actual electrode with its properly averaged surface roughness and field penetration effects). The inner Helmholtz plane (IHP) is taken as the plane of charge centroids of ions at kink sites, corresponding conceptually to the plane of charge centroids of surface (adsorbed) charges in the aqueous electrolyte case. For simplicitly, no distinction will be made here between the positions of Ag^+ and Cl^- ions on kink sites, allowing a single IHP to be employed. This approximation will be eliminated in later work. Finally, the outer Helmholtz plane (OHP) is taken to be the plane of charge centers of the first layer of the crystal, here the plane where vacancies and interstitials may be considered to still reside in the crystal, rather than at surface kink sites. We ignore (or average) the small differences between the position of this first plane for interstitials and for vacancies.

In addition to the bulk dielectric constant, we have also defined effective dielectric constants for the ESP–IHP region (thickness β) and the IHP–OHP region (thickness γ). The theoretical basis for the selection of effective dielectric constants has been extensively examined for the case of aqueous electrolyte,[24,26–28] and there includes contributions from the orientation of water

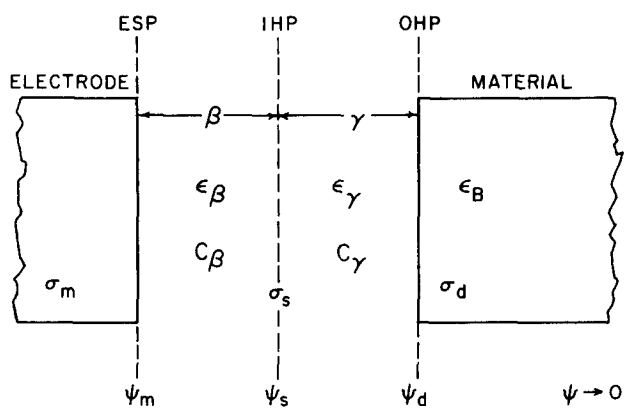

FIG. 7. Definitions of various quantities in the idealized electrode-interphase area.

molecules. Here one would expect the main contribution to the effective inner layer dielectric constants to arise from electronic polarization of the surface ions and thus one would expect ϵ_β and ϵ_γ to be probably no larger than n^2, the index of refraction squared, about 4 for AgCl. We shall take $\epsilon_\beta = \epsilon_\gamma \equiv \epsilon_A$ in the present work in view of the appreciable uncertainties of these quantities. The quantity ϵ_A is obviously best determined experimentally. Armstrong *et al.*[29] have derived a value of 2.8 from experiment for the interphase between Ag_4RbI_5 and Pt, a situation in which only the silver ion is mobile, as it is here in the surface region of AgCl. They state also that this value is in reasonable agreement with expectation. Here, for illustrative purposes, we shall use a field and temperature independent value of 3, realizing that the optimum value probably falls somewhere between 2 and 4. A more precise approach which we plan to follow in subsequent work is to derive an occupation and field dependent ϵ_A using a discrete-entity treatment[24,26,30] which accounts separately for the polarizabilities of both Ag^+ and Cl^- ion species at surface kink sites.

There is also some uncertainty in what values to employ for β and γ. For β we shall use the radius of a Ag^+ ion (1.26 Å) plus 0.5 Å to allow for field penetration in the metal electrode.[31,32] The proper value for γ will depend somewhat on the type of crystal surface plane considered. Here, we shall take γ as the sum of a Ag^+ radius and a Cl^- radius (1.81 Å) as is appropriate for an unrelaxed [100] surface. These considerations lead to values of the inner layer integral capacitances C_β and C_γ of about 15 and 8.7 $\mu F/cm^2$. We shall use these values in the rest of this paper. Note that their series combination $C_{\beta\gamma}$ is about 5.51 $\mu F/cm^2$.

In treating a superionic conductor situation where no separate surface charge layer (IHP) was assumed to be present, Armstrong[33] has considered the entire electrical double layer region to be restricted to the space between the electrode and the first complete layer of the crystal lattice and thus associated with a low dielectric constant. For a very high δ situation ($\delta \sim 0.5$) he has taken the total differential capacitance of the system C_D as in fact a compact layer capacitance equivalent to the present C_β, i.e., the capacitance of a parallel plate capacitor with plate separation equal to that between first-layer charge centers and the electrode. He states that this capacitance can never exceed ≈ 50 $\mu F/cm^2$. For a thickness of 1.26 Å (no allowance for field penetration into the metal electrode) and an effective dielectric constant of 3, however, the capacitance is only 21 $\mu F/cm^2$, so the value of 50 may well be an overestimate. Armstrong *et al.* actually derived a value for the inner layer capacitance of 20 $\mu F/cm^2$ from experimental measurements using a Pt electrode.[29] For those of the following calculations where no surface charge is assumed to be present or possible, we shall take the effective separation between the electrode and the surface of the crystal as leading to $C_\beta = 15$ $\mu F/cm^2$ and thus will take $C_\gamma = \infty$. Note that this situation is not the same as the $\sigma_s = 0$, zero surface charge, configuration associated with equal and nonzero numbers of Ag^+ and Cl^- ions at surface kink sites; for such a situation both C_β and C_γ are still finite. They remain independent of Γ_2 because of our assumption of constant ϵ_A.

Armstrong[33] considers the diffuse double layer space charge region to be negligible in his high δ situation because L_D is always less than the size of an atom in such superionic conductors. We shall continue to employ a continuum approximation for the diffuse layer in the present work, however, since for most materials there are many crystal planes within a Debye length over a wide temperature range. For example $L_D \sim 100$ Å at 500 K for AgCl. It has dropped to about 10 Å by the melting point, however, and a discrete, multilayer treatment of the diffuse region would then be more appropriate than the present continuum one. We plan to develop in later work a consistent discrete treatment of both surface and diffuse space charge regions. Even in the neighborhood of the melting point and above, however, our present combined discrete/continuum model will not usually be a very poor approximation as far as overall capacitance C_D is concerned because the potential difference across the diffuse region will often be only a small fraction of the total applied. This means that the diffuse region capacitance, which we shall designate C_{D0} hereafter, is usually much larger than C_D and thus, even if it is a poor approximation, will then not affect C_D appreciably.

In the present work we are concerned only with conditions at the blocking electrode and its neighborhood in the material of interest and thus take the second electrode to be ohmic, an infinite distance to the right, and take the zero of potential at this point. There is no bulk or geometric capacitance C_g for such a system. For completeness, however, and for use in later work, we have actually carried out the analysis of Appendix A for finite length. At $X = L$, there is present an ohmic electrode, one with an infinite recombination rate surface which ensures that the charge density $\rho \equiv e(c_2 - c_1)$ vanishes there. Nevertheless, for $L < \infty$, there will be a charge σ_L on this electrode. This charge will aproach zero as $L \to \infty$. But for $L < \infty$, it is σ_L that ensures that C_g is nonzero as it must be. Of course, in actual practice it is not possible to place the right-hand electrode at $X = \infty$. Therefore it is of interest to inquire how large $L \equiv l/L_D$ should be to ensure that conditions at the blocking end of the system are virtually the same as they would be with $L = \infty$. We shall explore this matter in greater detail, along with the way C_g appears in the equilvalent circuit in subsequent work. Here it is sufficient to remark that in a situation with nonzero surface charge at the blocking electrode, for $T = 500$ K and $\Gamma_s = 10^{14}$ sites/cm^2, ψ_m, ψ_s, ψ_d, σ_s, and σ_m at the blocking end are the same to three or more decimal places for $L = 3$ as for $L = \infty$. Incidentally, we assume that there is a rapid charge transfer reaction at the ohmic electrode which may be taken as a parent-ion type and thus that there is no potential drop between the end of the bulk material and the ohmic electrode. Thus, any capacitative effects which might possibly be present at this electrode are shorted out by the very small ($\to 0$) reaction resistance there.

For simplicity, we have implicitly assumed that the

binding of a Ag^+ ion at a surface kink site (next to a Cl^- at a jog) increases Γ_2 by one unit. While it certainly adds one unit of charge to σ_s, it is often considered to add to the surface two positive units, each of charge $e/2$. Consider a line of several alternating Ag^+, Cl^- ions on the surface, beginning with a Cl^- at one jog and ending with an Ag^+ at a second jog, so that the entire line protrudes from an otherwise uniform ledge. The line is then neutral. The addition of an Ag^+ next to the end Cl^- leaves the sequence with an Ag^+ at each end. Since only a single positive charge was added, one can consider that the two equivalent end Ag^+ ions each have a charge of $e/2$. On this picture we can interpret the equal number of Ag^+ and Cl^- ions on the surface at $\sigma_s = 0$ as Γ_s occupied positive kink sites of charge $e/2$ and Γ_s occupied negative kink sites of charge $-e/2$. The bookkeeping is independent of these interpretations.

For convenience, we shall continue to deal with quantities such as Γ_2 which count elements by full rather than half-charges. Then, as usual, there is a maximum of Γ_s positive Ag^+ ions possible at kink sites for given Γ_s. If one could close-pack Ag^+ ions on a smooth surface, one would obtain the purely steric limit $\Gamma_s \simeq 7.3\times10^{15}$ charges/cm^2. Trautweiler[34] has discussed the possibility of a maximum number of 10^{15} cm^{-2} Br^- ion sites on a AgBr surface. We shall only consider a maximum value of Γ_s for the present calculations for AgCl of 10^{14} cm^{-2}, recognizing that a somewhat larger value may, in fact, be possible on some crystal faces with specified degrees of roughness. Although we take Γ_s as independent of temperature and applied potential difference as have earlier writers in this field, there may be some such dependence. In particular, the high fields present in the inner region when $\Gamma_2 \cong \Gamma_s$ may cause some reconstruction of the surface, making it rougher and actually increasing Γ_s. We shall neglect any such possibility herein.

B. Potential and charge relations

Since $C_\beta \equiv \epsilon_A/4\pi\beta$ and $C_\gamma \equiv \epsilon_A/4\pi\gamma$, we may introduce for convenience the normalized quantities

$$\lambda_\beta \equiv C_{\beta N}^{-1} \equiv C_d/C_\beta = (\epsilon_B/\epsilon_A)(\beta/L_D) \tag{41}$$

and

$$\lambda_\gamma \equiv C_{\gamma N}^{-1} \equiv C_d/C_\gamma = (\epsilon_B/\epsilon_A)(\gamma/L_D)\ . \tag{42}$$

For a Frenkel defect material let us define

$$Q_m + Q_s \equiv -Q_d \equiv F(\phi_d) \equiv \mathrm{sgn}(\phi_d)\,[\delta^{-1}\ln\{1+R_2(\phi_d)\}]^{1/2}\ , \tag{43}$$

where R_2 is defined in Eqs. (26)–(28). The appearance of $\mathrm{sgn}(\phi_d)$ in Eq. (43) ensures that the signs of charges and associated potentials are consistent. We obtain the same diffuse region result as before, with ϕ_e now replaced by ϕ_d, because Appendix A shows that even when surface charge and an electrode are simultaneously present, free energy minimization still leads to the same expression for the charge distributions as that discussed in Sec. II A (see Eq. 8). The function $F(\phi_d)$ represents the negative of the integrated space charge in the material for the $L=\infty$ case, as shown in Appendix A. We shall only consider this case hereafter in this paper.

Now simple electrostatics leads to the following (normalized) potential relations, well known in the aqueous electrolyte area[24,27,35,36]:

$$\phi_s = \phi_d + \lambda_\gamma[Q_m + Q_s] = \phi_d + \lambda_\gamma F(\phi_d) \tag{44}$$

and

$$\phi_m = \phi_s + \lambda_\beta Q_m\ . \tag{45}$$

But Eq. (15) may be rewritten as

$$Q_s = Q_{sm}\tanh\left[\frac{\phi_{s0}-\phi_s}{2}\right]\ , \tag{46}$$

which may be considered a function only of ϕ_d when Q_{sm} and ϕ_{s0} are known (see Eq. 43). Therefore,

$$Q_m = F(\phi_d) - Q_s \tag{47}$$

is also only a function of ϕ_d and it follows from (45) that ϕ_m is also such a function. Thus, given a value of ϕ_d one may first calculate ϕ_s, then Q_m, and finally ϕ_m. If the basic variable is taken as ϕ_d, no iteration is required to calculate all the other average potentials and charges. Of course, if one requires that Q_m, Q_s, ϕ_s, or ϕ_m remain fixed, it will be necessary to solve an implicit equation for the ϕ_d value consistent with the value held fixed. We shall use both approaches in the following work. The P–B case essentially corresponds to Eq. (47) with $Q_m \equiv 0$. The implicit equation thereby obtained is much simpler to solve accurately as a function of ϕ_d than of ω, as was done in Sec. IID [see Eq. (40)].

C. Consideration of the adsorption isotherm and adsorption capacitance

Equation (46) which is in the form of an adsorption isotherm, is ultimately derived from free energy minimization under the condition that there was a limited number of surface sites per unit area Γ_s for positive ions, each limited to single occupancy. Since these are essentially the assumptions of the Langmuir adsorption isotherm, it is worthwhile establishing a connection between the two approaches. We begin by considering three particular forms of Langmuir adsorption.

The Langmuir adsorption isotherm involves a Fermi–Dirac distribution function[8,9] and may be written for positive and negative surface charges as

$$N_s^\pm/N_{sm}^\pm = [1+\exp\{\Delta G^\pm/kT\}]^{-1}\ , \tag{48}$$

where N_{sm}^+ and N_{sm}^-, not necessarily equal, are the maximum surface concentrations allowable of positive and negative charges. The $\Delta G^\pm$'s are the standard free energies of adsorption referenced to the point at which $N_s^\pm/N_{sm}^\pm = 0.5$. Consider the special but representative case where $N_{sm}^+ = N_{sm}^- \equiv N_{sm}$ and $\Delta G^\pm/kT \equiv \mathcal{G}^\pm = \pm[\phi_\mu - \mathcal{G}_0]$, where ϕ_μ is a normalized potential-dependent quantity (a micropotential) and $\mathcal{G}_0$ is independent of potential. Let $\sigma_{sm} = eN_{sm}$ and $Q_{sm} \equiv \sigma_{sm}/\sigma_n$ here. Then (47) leads to

$$\begin{aligned} Q_s &= Q_{sm}[\{1+\exp(\mathcal{G}^+)\}^{-1} - \{1+\exp(\mathcal{G}^-)\}^{-1}] \\ &= Q_{sm}\tanh\left[\frac{\mathcal{G}_0-\phi_\mu}{2}\right]\ . \end{aligned} \tag{49}$$

Next, consider the usual aqueous electrolyte case

where only charges of one sign (here positive) are adsorbed. Therefore, take $\mathcal{G}^-$ very large and positive and $\mathcal{G}^+ = \phi_\mu - \mathcal{G}_0$. Then one readily finds that

$$Q_s = Q_{sm}[1+\exp(\mathcal{G}^+)]^{-1}, \tag{50}$$

and σ_{sm} is here taken as eN^+_{sm}, a positive quantity.

Finally, consider the case where $N^+_{sm} = N^-_{sm} \equiv N_{sm} \equiv \Gamma_s$, $\sigma_{sm} = e\Gamma_s/2$, $\Delta G^- = 0$, and $\Delta G^+ \neq 0$. Then one finds

$$Q_s = (e\Gamma_s/\sigma_n)[\{1+\exp(\mathcal{G}^+)\}^{-1} - \tfrac{1}{2}] = Q_{sm}\tanh(-\mathcal{G}^+/2). \tag{51}$$

But these assumptions correspond to our present Ag^+, Cl^- kink site situation. Comparison of (49) and (51) shows them to be of the same form and comparison of (46) and (51) leads to the identification

$$\mathcal{G}^+ \equiv \phi_s - \phi_{s0}. \tag{52}$$

Thus our earlier results are fully consistent with the Langmuir adsorption isotherm as they should be. Although the present $\mathcal{G}^+$ depends only on average potentials (such as ϕ_s, ϕ_d, or ϕ_m) the above derivation makes it clear that corrections for discreteness of charge effects which will slow down the approach to surface charge saturation because of repulsion between like charges, will lead to the replacement of ϕ_s in (51) and (52) by micropotential terms.[24,37,38] Such discreteness corrections will be nearly symmetrical in Q_s because to first order it will be as difficult to add the last charge per unit area to a set of $(\Gamma_s/2-1)$ unbalanced positive charges as it will be to remove the last positive charge per unit area from a set of $\Gamma_s/2$ negative charges. In future work we plan to show how discreteness effects will change our present results.

Now the normalized adsorption capacitance is defined as

$$C_{AN} \equiv -dQ_s/d\phi_s. \tag{53}$$

For the situations of both Eqs. (49) and (51), it is found to be of the form

$$C_{AN} = (Q_{sm}/2)\operatorname{sech}^2\left[\frac{\phi_s-\phi_{s0}}{2}\right] = (Q_{sm}/2)[1-(Q_s/Q_{sm})^2], \tag{54}$$

although the Q_{sm}'s differ by a factor of two in the two cases. In the present AgCl situation Q_{sm} is $e\Gamma_s/2\sigma_n = e\Gamma_s/2C_d V_T = (2\sqrt{\delta}H)^{-1}$. Note that C_{AN} reaches its maximum value $Q_{sm}/2$ at the point where $Q_s = 0$. If for the case of Eq. (50) we again take $\mathcal{G}^+ = \phi_\mu - \mathcal{G}_0 \to \phi_s - \phi_{s0}$, we find

$$C_{AN} = Q_{sm}\left[\frac{e^{\phi_s-\phi_{s0}}}{\{1+e^{\phi_s-\phi_{s0}}\}^2}\right] = (Q_{sm}/4)\operatorname{sech}^2\left[\frac{\phi_s-\phi_{s0}}{2}\right]. \tag{55}$$

But this $Q_{sm}/4 = e\Gamma_s/4\sigma_n$, the same as the $Q_{sm}/2$ of Eq. (53). Thus we see that although the isotherms differ, the capacitances which follow from them are of exactly the same form. The first form of Eq. (55) is well known in aqueous electrochemistry[39] and the second form has appeared before in ionic adsorption and in electronic surface state calculations.[40] An approach for electronic surface states equivalent to that of Eqs. (48) and (49) has been given by Davison and Levine.[41]

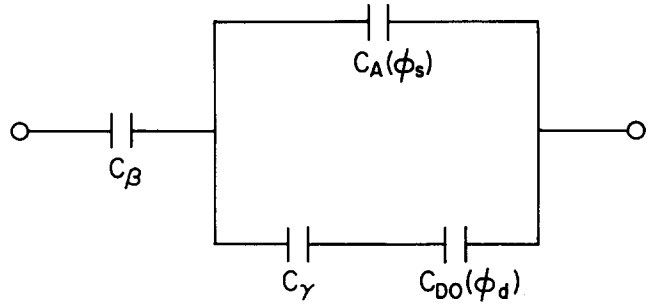

FIG. 8. Equivalent circuit for the total measurable differential capacitance C_D showing contributions from various sources.

D. The total differential capacitance C_D

Appendix B presents a derivation of the overall normalized differential capacitance C_{DN} of the system described in Fig. 7. The final result, Eq. (B8), appears reasonably complex but it leads to a particularly simple equivalent circuit Fig. 8 which we believe has not been obtained previously. We have indicated that two of the elements of this circuit depend explicitly on potential. Note that the maximum directly measurable value of C_D for this circuit is C_β, here taken as 15 μF/cm^2. Similarly, even if C_{DO} becomes very large, the maximum value for the branch in which it appears is C_γ, here 8.7 μF/cm^2. When $C_A \ll C_\gamma$, the overall maximum capacitance is just $C_D = C_{\beta\gamma} \equiv (C_\beta^{-1} + C_\gamma^{-1})^{-1}$.

It is particularly noteworthy and important that the exact analysis of Appendix B shows that the adsorption capacitance is in parallel with the series combination of C_γ and C_{DO}, *not* in series with C_{DO}. The capacitance C_A depends on ϕ_s (referenced to zero potential at the electrode at ∞) *not* on $(\phi_s - \phi_d)$, the usual assumption.[8,42] Thus, even a very small value of C_{DO} need not keep C_A from contributing its maximum effect. Further, the reaction plane is usually taken to be the IHP. If an electron can tunnel from the electrode to a Ag^+ ion at the IHP, an electron transfer reaction occurs. This process leads to a reaction resistance[14,43] in parallel with C_β, essentially shorting it out for dc response. We can take such a reaction into account for present purposes by choosing $C_\beta = \infty$. Then C_D will be dominated by C_A when it is much larger than C_γ, and very large values ($\gtrsim 100$ μF/cm^2) of C_D become possible, as is indeed observed for both aqueous and solid electrolyte situations. This situation will be considered in detail in future work which will include discreteness effects in adsorption.

The present C_A may be identified with the "adsorption pseudocapacitance" of aqueous electrolyte theory. It has been stated, however, that there can be no such capacitance for an ideally polarized (completely blocking) electrode, and that it only exists when a heterogeneous reaction occurs.[44] The above considerations suggest, however, that in the system considered here and others as well, a capacitance of the same form is indeed present under complete blocking conditions but is only fully expressed in C_D when an electrode reaction occurs and C_β is essentially shorted. When Γ_s is large, $(C_A)_{max} = e^2\Gamma_s/4kT$ may be very substantial. Note that had C_A appeared in series with C_{DO}, as it does in earlier

treatments, the maximum value of C_D would be limited to the maximum of C_{DO} (a concentration dependent quantity) even when C_A was far larger.

The present equivalent circuit Fig. 8 involves a C_{DO} which is more accurate than the conventional Gouy diffuse double layer capacitance because of our inclusion of ion size effects in the diffuse layer. C_{DO} therefore reaches a maximum at some ψ_d for any particular δ value, unlike the conventional C_{DO} which can increase without limit. Nevertheless, even the present calculation of C_{DO} needs improvement, improvement which we plan to provide in future work. It should be emphasized that the equivalent circuit of Fig. 8 includes potential dependent elements. The potential-charge relations of Eqs. (44)–(47) must be solved consistently as discussed to yield, given ψ_m, $C_A(\phi_s)$ and $C_{DO}(\phi_d)$. Then $C_D(\psi_m)$ may be calculated from the equivalent circuit or equivalently from Eq. (B8).

It should be mentioned that Armstrong[33] has considered a blocking-electrode, solid-electrolyte situation in which some cations may occupy "abnormal" positions, nearer the electrode than the first normal layer of cations and anions. In many respects our treatment of kink sites is analogous to his treatment of these positions. He assumes that there may be partial charge transfer between ions in abnormal positions and the electrode and finds the possibility of a large C_D which includes a large C_A contribution. We believe that even with partial charge transfer (partially covalent bonding), so long as the electrode does not permit a steady-state direct current, a proper consideration of C_β and C_γ would limit C_D to a maximum value of C_β as already discussed. Only in the presence of an electrode reaction, also considered by Armstrong, would C_A be able to make its full contribution to C_D. For this situation Armstrong essentially takes C_d infinite or replaces it by C_γ and does not consider C_β. Thus, for $C_\beta = \infty$, his result is consistent with ours (although he considers no explicit expression for C_A) provided C_{DO} is also taken as ∞. Some experimental situations may involve an appreciably greater degree of roughness of the electrode or crystal surface than assumed in Armstrong's or our work. A plausible equivalent circuit for such systems might involve the parallel combination of several sections, each of the form of Fig. 8.

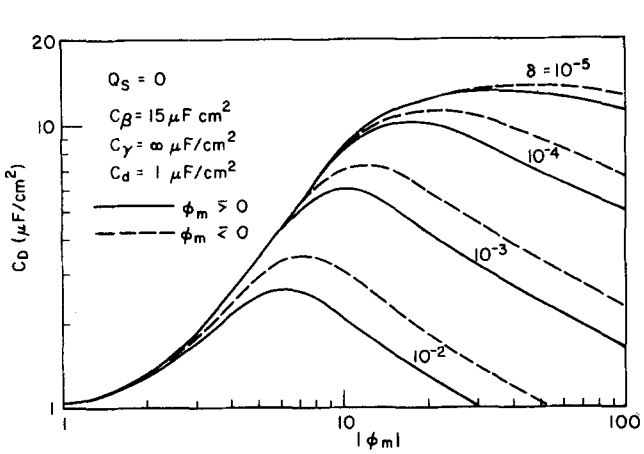

FIG. 9. C_D vs $|\phi_m|$, the normalized electrode potential for a single blocking electrode situation without separate surface charge possible for various values of δ.

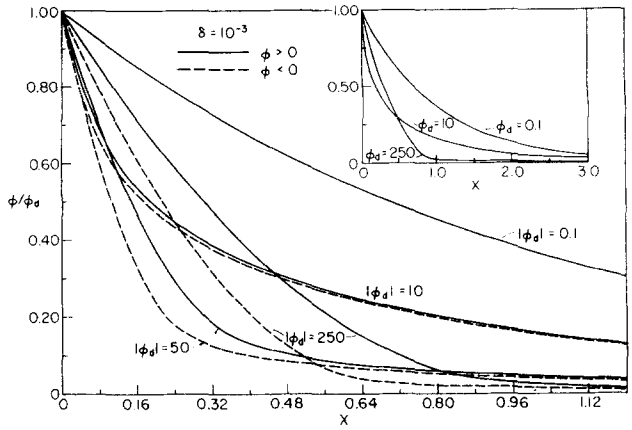

FIG. 10. The normalized potential ϕ/ϕ_d vs normalized distance X in the diffuse space charge region of the material for $\delta = 10^{-3}$.

E. Special situations

1. *Blocking electrode present, no surface charge*

This situation is the same as that considered in Sec. IIB except that C_β is here not infinite. The condition of no surface charge present (or assumed possible here) is achieved by taking $C_\gamma = \infty$, $\Gamma_s = 0$, and requiring that $Q_s = 0$ for any ψ_m value applied. Then $\psi_m \neq \psi_s \equiv \psi_d$. No implicit equation need be solved here if ϕ_d is taken as the independent variable. In the present situation the presence of a finite C_β value makes it somewhat inappropriate to plot a general C_{DN} vs $\phi_a \equiv \phi_m$. However, we have taken the explicit value $C_d = 1\ \mu F/cm^2$ in calculating the results of Fig. 9 so that here $C_D = C_{DN}$. Figure 9 may be compared with Fig. 1, but note that we use a logarithmic $|\phi_m|$ scale here instead of the linear scale used there. Comparison shows that the present curves exhibit smaller peaks than those with $C_\beta = C_\gamma = \infty$ and are, of course, limited so that $C_d \lesssim C_\beta = 15\ \mu F/cm^2$. These effects arise both because C_β is in series with C_{DO} here (see Fig. 8 with $C_A = 0$ and $C_\gamma = \infty$) and because C_β reduces $|\phi_d|$ so that $|\phi_d|$ is always less than $|\phi_m|$, making $C_{DO}(\phi_d)$ smaller than it would be if ϕ_m equaled ϕ_d.

2. *Diffuse layer behavior*

Consider now the diffuse space charge region in the material and recall that ϕ_d is the value of the normalized potential ϕ at the surface $X = 0$ and that $\phi \to 0$ as $X \to \infty$. Figure 10 shows some Frenkel defect results for ϕ/ϕ_d vs X for various values of ϕ_d. The main curves illustrate the behavior for $X \lesssim 1.2$, i.e., within 1.2 Debye lengths of the surface while the inset curves the response out to three Debye lengths. The rather odd behavior arises from the lattice gas limitations on mobile charge carrier concentrations. Note especially the progressive separation of the positive and negative curves for given ϕ_d as $|\phi_d|$ increases. Although these normalized curves show crossovers, none occurs when $\phi(X)$ rather than $\phi(X)/\phi_d$ is plotted.

The spatial dependence of the normalized charge densi-

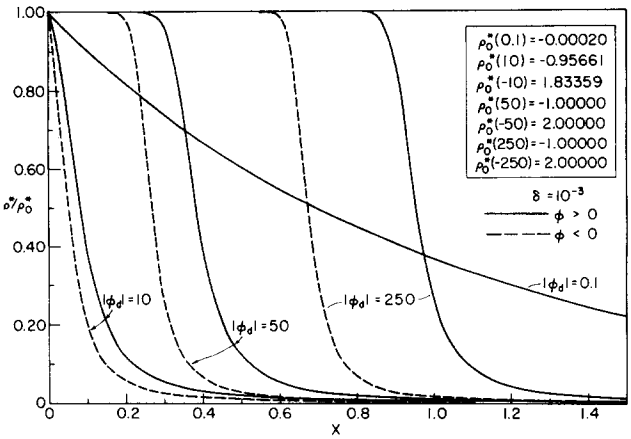

FIG. 11. The normalized charge density ρ^*/ρ_0^* vs X in the diffuse space charge region for $\delta = 10^{-3}$.

ty, $\rho^*(X) \equiv 2C_2 - C_1$ is shown in Fig. 11, where for easy comparison we have actually plotted ρ^*/ρ_0^*. Here ρ_0^* is the value of ρ^* at $X = 0$ for given ϕ_d (see values in inset of Fig. 11). For $|\phi_d|$ somewhat larger than $10\rho_0^*$ reaches its maximum value, $\rho_{0\max}^*$, that where $c_2 = 2N$ or $c_1 = N$, depending on the sign of ϕ_d. Figure 11 shows how the constant-ρ^* region grows as $|\phi_d|$ increases. The growth is quite slow and requires relatively large applied potentials. For example, at $T = 500$ K, $\phi_d = 250$ corresponds to $\psi_d \cong 10.77$ V. If L_D were 100 Å, the electric field in the region between the electrode and $X \sim 1$ would be of the order of 10^7 V/cm, possibly sufficient to cause breakdown. It should be remembered, as discussed in Sec. IIIA, that the present results for the diffuse layer only apply for many lattice planes contained in each Debye length and even then would be more accurately described by a modified lattice gas model, one which takes Coulombic interactions in the lattice planes parallel to the electrode into account. In the more accurate model it would be more difficult for $\rho^*(X)$ to reach the $\rho_{0\max}^*$ values shown here. It is likely that for reasonable values of ψ_d, $|\rho^*|$ will always be less than $|\rho_{0\max}^*|$. Finally, it should be pointed out that for any complete blocking situation with the series capacitance $C_\beta < \infty$, $|\psi_d|$ will be appreciably less than $|\psi_m|$. For example, with $C_\beta = 15\ \mu\text{F/cm}^2$, $C_\gamma = \infty$, $T = 500$ K and $Q_s = 0$, a ψ_d value of 2 V requires $\psi_m \cong 10.1$ V, and $\psi_d = 10$ V leads to $\psi_m \cong 30.3$ V.

3. $Q_m = 0$, surface charge present

This situation corresponds, except for $C_\gamma < \infty$, to the P–B no-electrode condition discussed in Sec. IID. When Q_m is held at zero, $\phi_m = \phi_s$ and the value of C_β is immaterial. Because we have dealt with average charges and ignored discreteness of charge effects, no self-imaging energy of an adsorbed charge in the conducting electrode has been included in the adsorption isotherm. Such inclusion would actually add a term nearly independent (to first order) of Q_s and T to ϕ_{s0}, a term of such sign that it always aided adsorption and led to more adsorption than would be present in its absence. This happens, of course, because the force between a charge moving to an adsorbed position and its image is always attractive. Because of the neglect of such imaging interactions, the moving of an uncharged conductor (the electrode) from $-\infty$ to its final position next to adsorbed surface charges causes no change in the energy of the system, and thus an uncharged electrode is, in this approximation, equivalent to none at all. We may therefore, compare present $Q_m = 0$ results with the earlier P–B ones to investigate the effect of removing the P–B idealization of implicitly taking $C_\gamma = \infty$. That the above neglect of imaging terms in adsorption is an approximation follows immediately from a well-known theorem of electrostatics, namely that the introduction of an uncharged conductor into the field of a fixed set of charges lowers the total energy of the field. We shall remove this approximation in later work.

The imposition of the $Q_m = 0$ condition generally requires that Eq. (47) be solved by iteration to obtain a consistent ϕ_d. For $Q_m = 0$ one obtains,

$$F(\phi_d) = -Q_{sm} \tanh\left[\frac{\phi_d - \phi_{s0} + \lambda_\gamma F(\phi_d)}{2}\right], \tag{56}$$

with $Q_s = F(\phi_d)$. For $\Gamma_s \to \infty$ and therefore $Q_{sm} \to \infty$, the tanh term must approach zero; thus in the case of very large Q_{sm} the tanh may be expanded and approximated by the first term in its series expansion. Then one obtains, on solving for $F(\phi_d)$,

$$F(\phi_d) \cong (Q_{sm}/2)\left[\frac{\phi_{s0} - \phi_d}{1 + \lambda_\gamma(Q_{sm}/2)}\right], \tag{57}$$

a result which reduces, when $Q_{sm} \to \infty$, to

$$Q_s = F(\phi_d) = C_{\gamma N}[\phi_{s0} - \phi_d], \tag{58}$$

an implicit equation for ϕ_d. This result yields, using Eq. (44), $\phi_s = \phi_d + \lambda_\gamma C_{\gamma N}(\phi_{s0} - \phi_d) \equiv \phi_{s0}$. Note that in this limit Eq. (58) shows that $\sigma_s = C_\gamma(\psi_s - \psi_d)$ where $(\psi_s - \psi_d)$ is just the p.d. across C_2.

Results are not the same for $Q_{sm} \to \infty$ in the Kliewer-Koehler, P–B situation where $\lambda_\gamma = 0$. Then solution of Eq. (56) or (57) leads to $\phi_d = \phi_{s0}$, yielding

$$Q_s = F(\phi_{s0}). \tag{59}$$

Since $\phi_s = \phi_d = \phi_{s0}$ here, one sees that $\phi_s = \phi_{s0}$, independent of λ_γ even though Q_s does depend on λ_γ. As an illustration of the differences, take $T = 500$ K, $\Gamma_s \to \infty$, and $C_\gamma = 8.7\ \mu\text{F/cm}^2$. Then $C_{\gamma N} \cong 6.237$ and iterative solution of Eq. (58) yields $Q_s \cong 17.20$. For the $\lambda_\gamma = 0$ case, Eq. (59) leads to $Q_s \cong 67.88$. In both cases $\phi_s = \phi_{s0} \cong 8.456$ and thus $\psi_s = \psi_{s0} \cong 0.364$ V.

Figure 12 compares P–B results for $\psi_s(T)$ (corresponding to the $\phi_s(T)$ curves of Fig. 4) with those obtained when $\lambda_\gamma > 0$ and thus $C_\gamma < \infty$. The top dotted curve shows the $\Gamma_s = \infty$, $\psi_s = \psi_{s0}$ results discussed above, independent of C_γ. The other curves show, however, that for $\Gamma_s = 10^{14}\ \text{cm}^{-2}$ the value of C_γ has a large effect on $\psi_s(T)$. In particular, the $C_\gamma = 8.7\ \mu\text{F/cm}^2$ curve, which should be close to the most appropriate value, is very different from the P–B $C_\gamma = \infty$ curve and lies much nearer the $\Gamma_s = \infty$ curve. It thus appears that interpretation of $\psi_s(T)$ data (perhaps obtained by the vibrating capacitor technique[12]) implicitly or explicitly assuming $C_\gamma = \infty$ would lead to quite inaccurate values of $S_-(T)$. As Fig. 13 demonstrates, however, the situation is much less serious for small Γ_s such as $10^{12}\ \text{cm}^{-2}$. Danyluk and

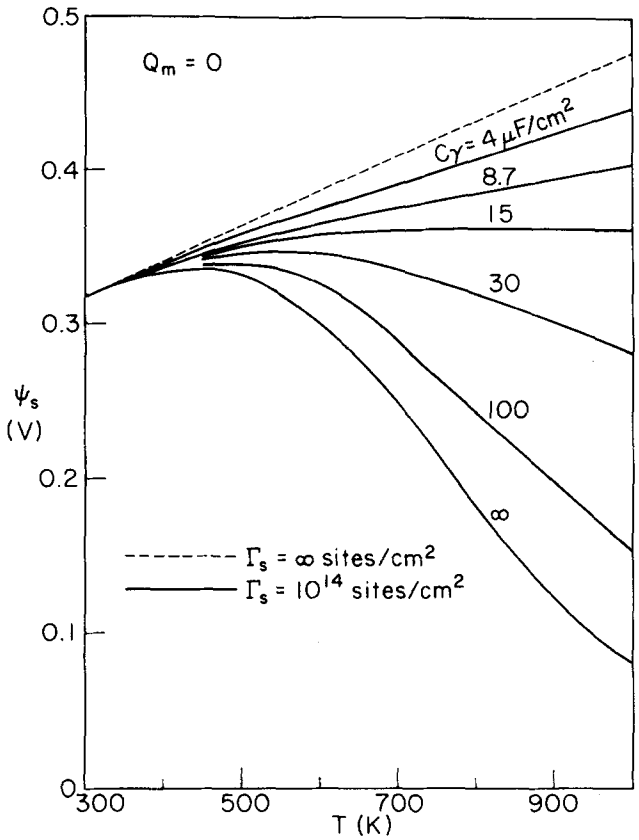

FIG. 12. Surface potential ψ_s vs T for a situation without electrode and various values of the inner region capacitance C_γ.

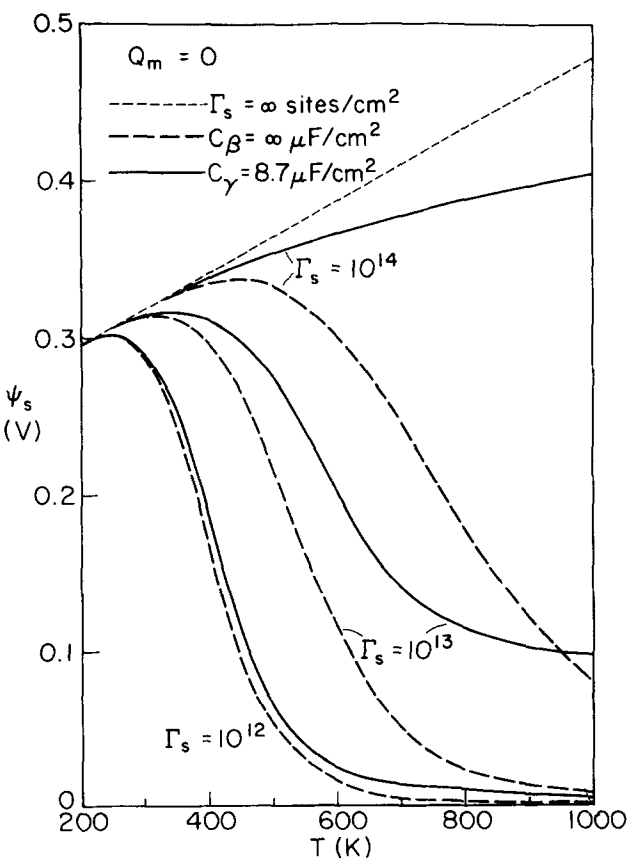

FIG. 13. Surface potential ψ_s vs T for no electrode and various values of Γ_s.

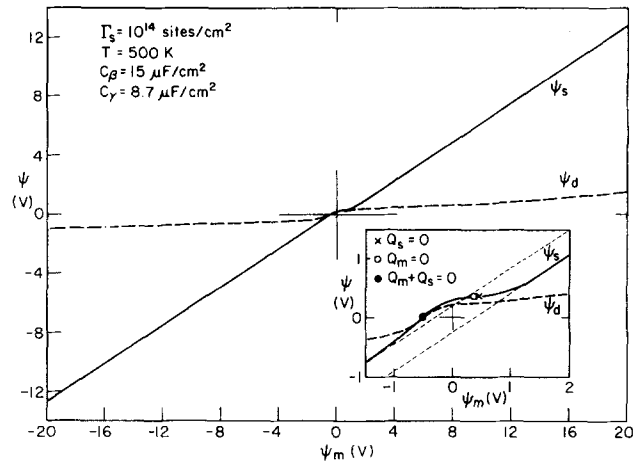

FIG. 14. The dependences of ψ_s and ψ_d on electrode potential ψ_m for $\Gamma_s = 10^{14}$ sites/cm^2 and surface charge and blocking electrode both present.

Blakely[12] indeed found strong differences between their vibrating capacitor results for different AgCl surface orientations (perhaps reflecting in part different Γ_s values) but did not quote any Γ_s or σ_s values. Therefore, it is not possible to estimate how much their derived ΔS_v results may be in error because of their $C_\gamma = \infty$ assumption.

F. Some potential and charge results

From now on, we shall consider an interface involving an electrode and possible surface charge. Figure 14 shows ψ_s and ψ_d vs ψ_m for typical values of Γ_s, T, C_β, and C_γ. Because of the strongly nonlinear dependence of $C_{DO}(\psi_d)$ on ψ_d, this quantity grows much less rapidly with ψ_m than does ψ_s. The interesting behavior in the small $|\psi_m|$ region is shown expanded in the inset. Because $\phi_{s0} \neq 0$, $\psi_s \neq 0$ when $\psi_m = 0$ and ψ_m must be negative to force ψ_s to zero. Values of ψ_s for which various charges are zero are indicated on this ψ_s curve. Incidentally, for $|\psi_d| \gtrsim 0.4$ V, one has $R_2 > 0.1$, so that expansion of $\ln(1+R_2)$ in (42) begins to become a poor approximation. Some further numerical results are presented in Table I. Line 1 corresponds to the flat-band condition, that where there is no diffuse layer space charge. Because of adsorption, this by no means corresponds to the point of zero charge (pzc), that where $\sigma_m = 0$. The σ values in the table may be converted to normalized Q values by the relation $Q = \sigma/\sigma_n$, where σ_n is here 0.0601 μC/cm^2. Since $\psi_s = 0$ for line 1, the results given there are all independent of λ_γ. The ψ_m value is given by $\psi_m = -(e\Gamma_s/2C_\beta)\tanh(\phi_{s0}/2)$. This

TABLE I. Values of ψ_m which lead to significant values of other quantities for $\Gamma_s = 10^{14}$ sites/cm^2 and $T = 500$ K. Also $C_\beta = 15$ μF/cm^2; $C_\gamma = 8.7$ μF/cm^2; $\sigma_{sm} \cong 8.0109$ μC/cm^2; and $\psi_{so} \cong 0.3643$ V.

	ψ_m (V)	ψ_s (V)	ψ_d (V)	σ_m (μC/cm^2)	σ_s (μC/cm^2)	$(\sigma_m + \sigma_s)$ (μC/cm^2)
1	−0.534	0	0	−8.008	8.008	0
2	0	0.298	0.215	−4.468	5.190	0.722
3	0.354	0.354	0.241	0	0.981	0.981
4	0.433	0.364	0.246	1.034	0	1.034
5	0.513	0.375	0.250	2.069	−0.981	1.088

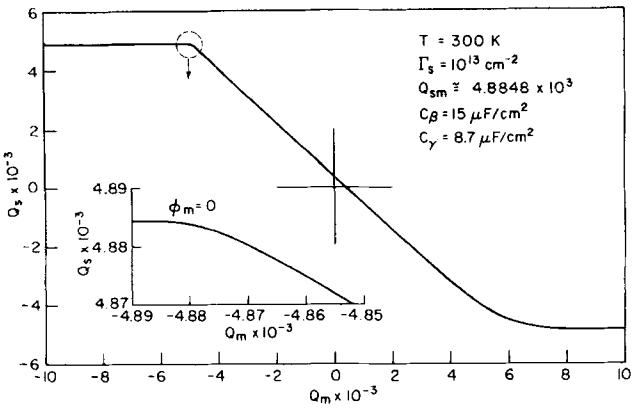

FIG. 15. Adsorption isotherm $Q_s(Q_m)$ for $T = 300$ K and $\Gamma_s = 10^{13}$ sites/cm^2.

quantity, rather than ψ_{s0} itself, plays somewhat the same role here as the ψ_D constant potential shift introduced in Sec. IIC, but this ψ_m is not necessarily constant. In the present instance the tanh term is very close to unity, so ψ_m is essentially dependent only on Γ_s and C_β. For $\Gamma_s = 10^{15}$ cm^{-2}, possibly not realizable, ψ_m would achieve the large value of -5.3 V.

Line 2 shows the results for zero p.d. between the working electrode and that at $x = \infty$. To achieve this condition one will generally have to compensate for any contact p.d. between the blocking and ohmic electrodes with an external series voltage source of the correct magnitude. It will usually be convenient to take the effective applied p.d., ψ_a, with reference to this balancing source so that $\psi_a = \psi_m$.

Line 3 shows conditions for $\sigma_m = 0$, already discussed to some extent in Sec. IIIE3 where we took $Q_m = 0$. This is the pzc in aqueous electrolyte terminology. Here $\phi_m = \phi_s = \phi_d + \lambda_\gamma F(\phi_d)$ where ϕ_d is the consistent solution of Eq. (56). Next, line 4 gives the $\sigma_s = 0$ results; here $\psi_s = \psi_{s0}$ and $\phi_m = \phi_{s0} + \lambda_\beta F(\phi_d)$ and $\phi_d = \phi_{s0} - \lambda_\gamma F(\phi_d) = \phi_{s0} - \lambda_\gamma Q_m$. Thus $\psi_d = \psi_{s0} - C_\gamma^{-1}\sigma_m$. Finally, line 5 shows results for a σ_s equal and opposite to that of line 3.

Figure 15 shows a typical adsorption isotherm $Q_s(Q_m)$. One of the most striking results is that the curve does not pass through the origin (see also lines 3 and 4 of Table I). Thus there is surface charge present even at the pzc. In the aqueous electrolyte area this behavior is known as specific or superequivalent adsorption.[45] There is a limited region exhibiting adsorption of positive charge even when the electrode is itself positive. It is usual to ascribe specific adsorption to image forces and to the difference in chemical bonding and dispersion forces between the bulk of the material and the interfacial layer.[45] Here the former are neglected while the latter are accounted for in an approximate and formal way in the thermodynamic conditions which lead to a nonzero ϕ_{s0} [see Eq. (16)]. Had we included a more accurate description of some or all of the forces mentioned above, it would have added a nearly temperature-independent positive constant to the present temperature-dependent value of ψ_{s0}. Then ψ_{s0} would be larger than 0.364 V and the region over which Q_s and Q_m would have the same sign would be larger.

Another remarkable feature of the curve of Fig. 15 is the presence of a large region where $Q_s(Q_m)$ is linear. This region extends very nearly to the point where Q_s reaches its positive saturated value of Q_{sm}. The region encompassing the transition to positive saturation is shown greatly expanded in the inset. In the present treatment, which includes no Coulombic repulsion terms in the surface adsorption layer at the IHP, slowing the approach to either positive or negative saturation, it is evidently considerably easier to reach positive than negative saturation. The inclusion of discreteness-of-charge repulsion terms may be expected to cause the approaches to positive and negative saturation to become more symmetrical.

G. Total differential capacitance results

In the present model, both the capacitances C_{DO} and C_A of Fig. 8 are temperature as well as potential dependent. Now as Eq. (54) shows, C_A is a maximum at the $Q_s = 0$ point. Therefore, in Fig. 16 we have plotted C_D vs $10^3/T$ at this point. The curves for various values of Γ_s should therefore indicate nearly the maximum of C_D as well. As we have seen earlier, however, a temperature-dependent ψ_m is required in order to satisfy the $Q_s = 0$ condition. The actual values of ψ_m, $\psi_s = \psi_{s0}$, and ψ_d are plotted in the bottom region of the graph. Because $Q_s = 0$, they are independent of Γ_s, although

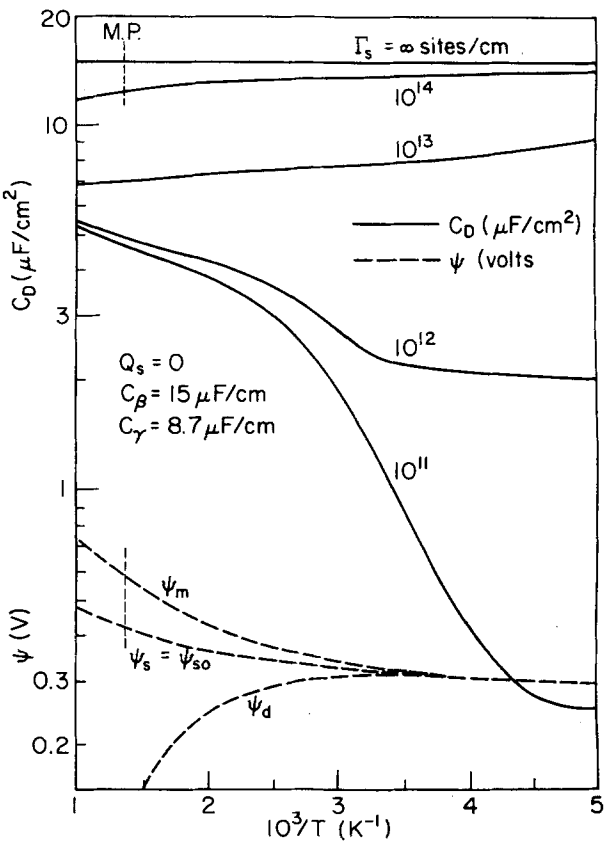

FIG. 16. C_D vs $10^3/T$ at the $Q_s = 0$ point with surface charge possible for various Γ_s values. Corresponding temperature dependences of ψ_m, ψ_s, and ψ_d also shown.

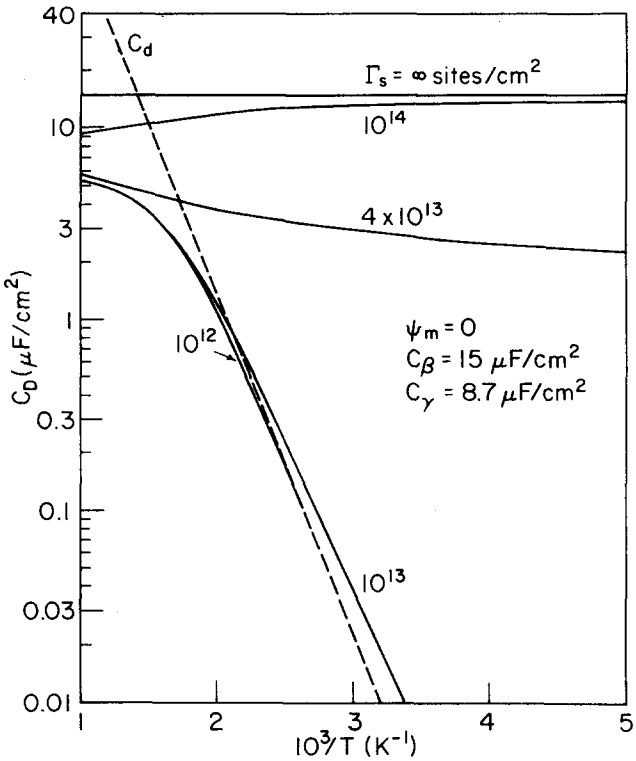

FIG. 17. C_D vs $10^3/T$ for $\psi_m = 0$ and various Γ_s values.

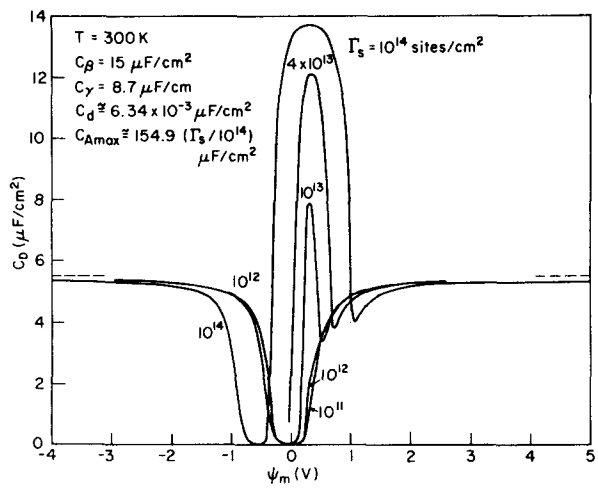

FIG. 19. C_D vs ψ_m for $T = 300$ K and various Γ_s values.

of course, C_D is not. These results show that depending on Γ_s, it is possible for C_D to either increase or decrease with temperature.

Although the curves of Fig. 16 are useful in giving an indication of how the maximum C_D depends on temperature, they do not correspond to measurements at constant ψ_m. To illustrate some of the behavior possible with constant ψ_m, Fig. 17 shows results for ψ_m fixed at zero. We see that for $\Gamma_s \lesssim 10^{13}$ cm^{-2}, $C_D \sim C_d$ until the high temperature region is reached where C_D approaches $C_{\beta\gamma}$. Clearly, C_A makes little contribution for these values of Γ_s at $\psi_m = 0$. On the other hand, for $\Gamma_s \gtrsim 4 \times 10^{13}$ cm^{-2}, C_A begins to play an appreciable role and entirely changes the character of the temperature dependence. Note that in both Figs. 16 and 17, the $\Gamma_s = \infty$ cm^{-2} curve is just that for $C_D = C_\beta$ at all temperatures. Here C_A is so large that C_β entirely dominates the equivalent circuit.

We turn now to the potential dependence of C_D at constant temperature. Figures 18 and 19 show results for two different temperatures and various Γ_s values. Since $(C_{AN})_{max} = Q_{sm}/2$, $C_{Amax} = e\Gamma_s/4V_T$, and is hence inversely proportional to T. The values of C_{Amax} are indicated on Figs. 18 and 19 and reach large values for $\Gamma_s \gtrsim 10^{14}$ cm^{-2}. But unless the electrode is not completely blocking and an electrode reaction occurs, these large values of C_A which may exceed 100 μF/cm^2, appear in series with C_β and as usual, C_D cannot exceed $C_\beta = 15\ \mu F/cm^2$. Clearly, however, the larger Γ_s and C_{Amax}, the broader the adsorption peak. For Γ_s values of 10^{12} cm^{-2} or less, adsorption makes very little contribution to the overall capacitance of the system. The maxima of these C_D curves occur very nearly at the $Q_s = 0$ point, where C_A is itself a maximum. Therefore, the ψ_m value at the

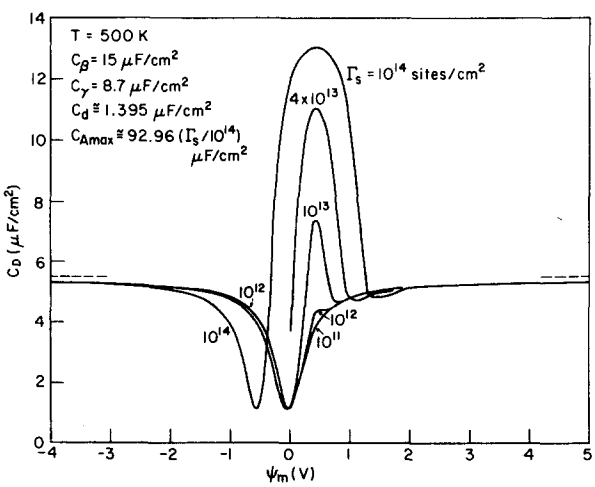

FIG. 18. C_D vs ψ_m for a typical AgCl situation, $T = 500$ K, and various Γ_s values.

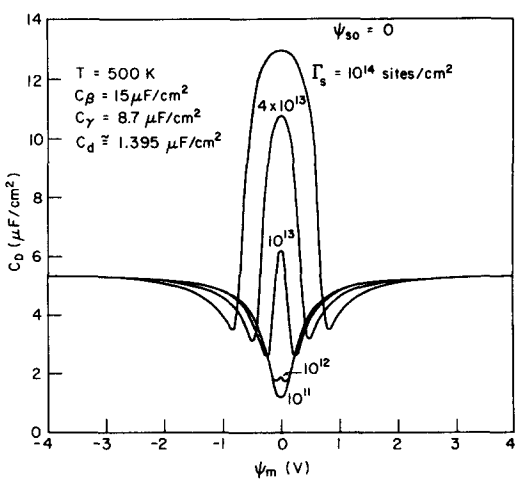

FIG. 20. C_D vs ψ_m for $T = 500$ K, $\psi_{so} = 0$, and various Γ_s values.

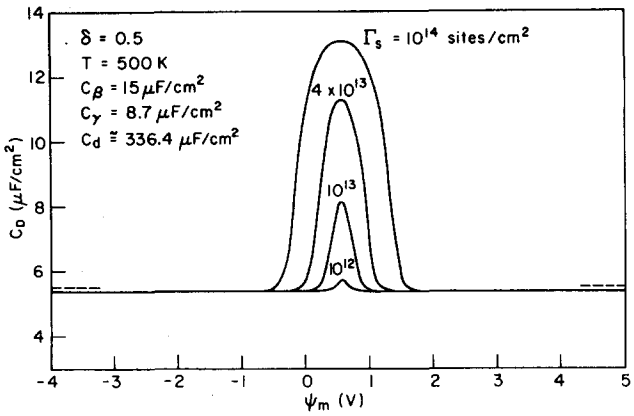

FIG. 21. C_D vs ψ_m for $T=500$ K; like Fig. 18 except that $\delta=0.5$.

maxima is approximately $\psi_m=\psi_{s0}+(\sigma_m/C_\beta)$, 0.433 V for $T=500$ K.

The minima of the curves of Figs. 18 and 19 occur at the flat-band condition, that where $\psi_d=0$ (see line 1 of Table I). The nearly symmetric rising curves on either side of the minima are the usual Gouy diffuse double layer C_{DO} capacitance rises, modified here by the displacement from $\psi_m=0$ and the present lattice gas treatment of the diffuse layer. Some of the main differences between the results of Figs. 18 and 19 arise from the difference in $C_{DO\min}\cong C_d$ values for the two temperatures considered. It is clearly the displacement of the minima and maxima of these curves from the $\psi_m=0$ point (because $\psi_{s0}\neq 0$) which keeps C_A from dominating C_{DO} near its minimum and allows the Gouy regions to appear even for large Γ_s values here.

It is therefore of interest to examine what happens when ψ_{s0} is actually taken zero. The same situation as that taken for Fig. 18 is assumed but ψ_{s0} is arbitrarily set to zero. Results appear in Fig. 20. They indicate how the adsorption capacitance keeps the minimum of C_{DO} from appearing until Γ_s is less than 10^{12} cm^{-2}. These curves are very nearly but not quite symmetrical around $\psi_m=0$.

Finally, what changes occur when δ is much larger, as in a superionic conductor? To get some feel for behavior with large δ, we have taken our $T=500$ K results for AgCl and arbitrarily changed δ from its original value of about 8.6×10^{-6} to 0.5. All other δ-dependent quantities are changed correspondingly. Then C_{DO} is large over the entire p.d. range of interest, and C_{DO}^{-1} may be neglected compared to C_γ^{-1}. Some results are shown in Fig. 21. As expected, they show that $C_D\cong C_{\beta\gamma}$ except where C_A is important. Further, there is a slight shift of the value of ψ_m at the maxima to larger voltages than those appearing in Fig. 18.

GLOSSARY OF MAJOR SYMBOLS

A. Major subscripts

a	Applied, as in applied p.d.
e	Effective, as in effective p.d.
i	1, 2. The value 1 designates a negative charge carrier or a Schottky defect, while 2 designates a positive charge carrier or a Frenkel defect situation.
j	d (diffuse), A (adsorption), D (differential), DO (diffuse layer alone).
k	d (diffuse), m (metal electrode), s (surface).
0	Bulk.
L	Left electrode (when two blocking electrodes are present).
N	Normalized Capacitance: $C_N\equiv C/C_d$.
R	Right electrode (when two blocking electrodes are present).

B. Major symbols

a_i	Activity associated with c_i.
c_i	Charge carrier concentration.
c_{i0}	Value of c_i in the undisturbed bulk.
c_0	Common value of c_{10} and c_{20} when $z_1=z_2$.
e	Protonic charge.
k	Boltzmann constant.
l	Length of single crystal material.
l_1	$(\beta+\gamma)$.
s_i	1 for Schottky defects; $s_1=1$, $s_2=2$ for Frenkel defects.
x	Distance in crystal measured from beginning of diffuse region at the blocking electrode.
z_i	Valence number of charge carriers.
C_g	Geometric capacitance.
C_i	c_i/N_i.
C_j	Various capacitances per unit area.
C_β	Capacitance between ESP and IHP.
C_γ	Capacitance between IHP and OHP.
D_i	Diffusion coefficient of ith type of charge carrier.
E	Electric field.
$\mathcal{E}$	Normalized field: eL_DE/kT.
$F(\phi_d)$	$-Q_d$; see Eq. (43).
$\mathcal{G}_i$	$\Delta G_i/kT$.
$\mathcal{G}_+$	$\mathcal{G}_1+\mathcal{G}_2$.
$\mathcal{G}_-$	$\mathcal{G}_1-\mathcal{G}_2$.
ΔG_i	Free energies of formation of charged species.
H	$C_0V_T/e\Gamma_s=C_dV_T/\sqrt{\delta}$.
I_i	Conduction current density for ith species of charge.
L	l/L_D.
N_i	s_iN.

N	Common concentration of anion and cation sites.
Q_k	σ_k/σ_n; normalized charges.
Q_{sm}	σ_{sm}/σ_n; maximum normalized surface charge density.
R_i	Schottky or Frenkel parameter; Eqs. (23), (25′)–(28).
T	Absolute temperature.
T_i	Thermodynamic factor; $(c_i/a_i)(\partial a_i/\partial c_i)$.
V_T	Thermal voltage; kT/e.
X	x/L_D.
β	Distance between ESP and IHP; see Fig. 7.
γ	Distance between IHP and OHP, see Fig. 7.
ϵ_A	Dielectric constant in region between ESP and OHP.
ϵ_B	Dielectric constant in bulk of material in the low frequency limit.
λ_β	$C_{\beta N}^{-1} \equiv C_d/C_\beta$.
λ_γ	$C_\gamma^{-1} \equiv C_d/C_\gamma$.
δ	Fractional defect concentration in the bulk; c_0/N.
μ_{mi}	Mobility of ith charge species.
ρ	Volume concentration; $e(c_2 - c_1)$.
ρ^*	Normalized volume concentration; $(s_2 C_2 - s_1 C_1)$.
σ_k	Various charges per unit area.
σ_n	Normalizing surface charge density; $2ec_0 L_D \equiv C_d V_T$.
σ_{sm}	Maximum net surface charge density; $e\Gamma_s/2$.
ϕ	ψ/V_T.
ψ	Local potential referred to zero potential at the ohmic electrode ($x \to \infty$).
ψ_{s0}	Value of surface potential ψ_s when $\sigma_s = 0$. See Eq. (16).
ψ_a	Applied p.d.
ψ_e	Effective p.d.
ω	$(\sigma_s/e\Gamma_s) = \sigma_s/2\sigma_{sm}$
Γ_s	Number per unit area of available surface sites for positive ions.
Γ_2	Number per unit area of surface sites filled with one positive ion per site.

APPENDIX A: FREE ENERGY MINIMIZATION

Kliewer and Koehler[3] and Poeppel and Blakeley[5] have minimized the free energy of a Frenkel defect single crystal in the absence of electrodes, without and with a limitation on surface charge density, respectively. Here we generalize to a finite length single crystal with one blocking and one ohmic electrode. The crystal is treated as a continuum, with the exception of the crystal surface plane near the electrode, for which we assume that there are only Γ_s possible sites for positive surface (adsorbed) charges as in the main text.

As in Fig. 7 let us take the beginning of the continuum (OHP) to be at $x = 0$ and the ohmic electrode at $x = l$, corresponding to $X \equiv l/L_D = L$. Then the IHP is at $x = -\gamma$ and the metal electrode at $x = -(\beta + \gamma) \equiv -l_1$.

On extending the P–B formalism[5] to the present situation, one finds that the Gibbs free energy (for unit area and constant pressure and temperature) is given by

$$G = W(l) + \int_0^l [c_1(x)\,\Delta G_1 + c_2(x)\,\Delta G_2 - TS_{cB}]\,dx - TS_{cS} + G_{el} - W_b \,. \tag{A1}$$

Here $W(l)$ is the binding energy of the crystal of length l without defects; ΔG_i is, as usual, the free energy of defect formation; and $W_b \equiv \sigma_m \psi_m$ is the work performed by an external battery in charging the electrodes. The potential of the blocking electrode ψ_m is taken with respect to $\psi = 0$ at $x = l$ and includes any contact p.d.'s present.

Now $S_{cB} = S_{cB}(c_i, N)$ is the standard[46] configurational entropy of the bulk defects per unit volume. It may be written as

$$S_{cB} = \left(\frac{k}{V_0}\right) \ln\left\{\frac{(NV_0)!}{[(N - c_1)V_0]!\,[c_1 V_0]!} \cdot \frac{(s_2 NV_0)!}{[(s_2 N - c_2)V_0]!\,[c_2 V_0]!}\right\} , \tag{A2}$$

where V_0 is the unit of volume and s_2 is the structure factor, equal to two for typical Frenkel disorder. Similarly, the configurational entropy per unit area associated with the surface site occupation takes the form

$$S_{cS}(\Gamma_2, \Gamma_s) = \left(\frac{k}{A_0}\right) \ln\left\{\frac{(\Gamma_s A_0)!}{[(\Gamma_s - \Gamma_2)A_0]!\,[\Gamma_2 A_0]!}\right\} , \tag{A3}$$

where A_0 is the unit of surface area. Finally, $G_{el} \equiv G_{el}(\sigma_s, \psi_m, \rho)$ is the electrostatic free energy,[47] given by

$$G_{el} = \tfrac{1}{2}\left[\sigma_m \psi_m + \sigma_s \psi_s + \int_0^l \rho(x)\,\psi(x)\,dx\right] . \tag{A4}$$

Here the volume charge density is given by

$$\rho(x) = e\,[c_2(x) - c_1(x)] \,, \tag{A5}$$

and, as usual, $\sigma_s = e\,[\Gamma_2 - (\Gamma_s/2)]$.

From simple electrostatics, one finds that the potential within the compact double layer may be written

$$\psi(x) = \begin{cases} \psi_m & x \le -l_1 \\ \psi_m - \left(\dfrac{4\pi\sigma_m}{\epsilon_A}\right)(l_1 + x) & -l_1 \le x \le -\gamma \\ \psi_m - \left(\dfrac{4\pi}{\epsilon_A}\right)\{(\sigma_m l_1 + \sigma_s \gamma) + (\sigma_m + \sigma_s)x\} \,. & -\gamma \le x \le 0 \end{cases} \tag{A6}$$

On the inverval $0 \le x \le l$, ψ satisfies the Poisson equation

$$\frac{d^2\psi}{dx^2} = -\left(\frac{4\pi}{\epsilon_B}\right)\rho(x) , \tag{A7}$$

with the following boundary conditions:

$$\left.\begin{aligned} &\psi(0) = \psi_m - \left(\frac{4\pi}{\epsilon_A}\right)[\sigma_m l_1 + \sigma_s \gamma] , \\ &\psi'(0) = -\left(\frac{4\pi}{\epsilon_B}\right)(\sigma_m + \sigma_s) , \\ &\psi(l) = 0 , \\ &\psi'(l) = \left(\frac{4\pi}{\epsilon_B}\right)\sigma_l . \end{aligned}\right\} \tag{A8}$$

Here the prime denotes differentiation with respect to x.

The equilibrium values of $c_i(x)$ and σ_s at fixed pressure and temperature can be determined by requiring that G be a minimum with respect to independent variations. Using the variation operator δ (assumed to commute with differentiation[48]) and Sterling's approximation, one finds that (A1) leads to

$$\begin{aligned} \delta G = \int_0^l \Bigg\{ &\left[\Delta G_1 + kT \ln\left\{\frac{c_1(x)}{N - c_1(x)}\right\}\right]\delta c_1(x) \\ &+ \left[\Delta G_2 + kT \ln\left\{\frac{c_2(x)}{2N - c_2(x)}\right\}\right]\delta c_2(x)\Bigg\} dx \\ &+ \left(V_T \ln\left\{\frac{[\Gamma_s + (2\sigma_s/e)]}{[\Gamma_s - (2\sigma_s/e)]}\right\}\right)\delta\sigma_s + \delta G_{el} - \delta W_b , \end{aligned} \tag{A9}$$

where we have set $s_2 = 2$. Now from Eq. (A4) one obtains

$$\begin{aligned} \delta G_{el} = \frac{1}{2}\Bigg[&\left(\psi_m - \frac{4\pi\sigma_s\beta}{\epsilon_A}\right)\delta\sigma_m + \left(\psi_m - \frac{4\pi\sigma_m\beta}{\epsilon_A}\right)\delta\sigma_s \\ &+ \int_0^l \{\psi(x)\,\delta\rho(x) + \rho(x)\,\delta\psi(x)\}\,dx\Bigg] . \end{aligned} \tag{A10}$$

Next from Eq. (A7) and the identity

$$\phi_2 \nabla^2\phi_1 = \phi_1 \nabla^2\phi_2 + \nabla\cdot[\phi_2\nabla\phi_1 - \phi_1\nabla\phi_2] , \tag{A11}$$

one readily finds that

$$\begin{aligned} \int_0^l \rho(x)\,\delta\psi(x)\,dx = &\int_0^l \psi(x)\,\delta\rho(x)\,dx \\ &-\left(\frac{\epsilon_B}{4\pi}\right)\left[\frac{d\psi}{dx}\,\delta\psi - \psi\delta\left(\frac{d\psi}{dx}\right)\right]_0^l . \end{aligned} \tag{A12}$$

The boundary conditions (A8) allow the surface terms in (A12) to be evaluated, leading to

$$\delta G_{el} = \psi_m\,\delta\sigma_m + \psi_s\,\delta\sigma_s + \int_0^l \psi(x)\,\delta\rho(x)\,dx , \tag{A13}$$

where as usual, $\psi_s = \psi_m - (4\pi/\epsilon_A)\sigma_m\beta$. Equation (A9) may now be rewritten as

$$\begin{aligned} \delta G = \int_0^l \Bigg\{ &\left[\Delta G_1 + kT \ln\left\{\frac{c_1(x)}{N - c_1(x)}\right\} - e\psi(x)\right]\delta c_1(x) \\ &+ \left[\Delta G_2 + kT \ln\left\{\frac{c_2(x)}{2N - c_2(x)}\right\} + e\psi(x)\right]\delta c_2(x)\Bigg\} dx \\ &+ \left\{V_T \ln\left\{\frac{[\Gamma_s + (2\sigma_s/e)]}{[\Gamma_s - (2\sigma_s/e)]}\right\} + \psi_s\right\}\delta\sigma_s . \end{aligned} \tag{A14}$$

From total charge conservation, or equivalently, from the first integral of Eq. (A7), Gauss' law, one obtains the constraint

$$\sigma_m + \sigma_s + \sigma_d + \sigma_l = 0 , \tag{A15}$$

where

$$\sigma_d \equiv \int_0^l \rho(x)\,dx \tag{A16}$$

is the integrated space charge.

We shall now take the variations $\delta\sigma_m$ and $\delta\sigma_l$ to be zero. Our justification for this assumption is as follows. Consider first the usual situation in which a p.d. of say $\psi_m = \psi_{m1}$ is continuously applied to the system by means of an external battery. After sufficient time is allowed for equilibrium to become established, G is a minimum and all the charges have reached their final values. Alternatively, start with an uncharged systen and now apply a potential difference ψ_{m2} to the system for a fixed short time, then disconnect the battery and leave the blocking electrode open circuited and floating. A certain amount of charge will have been transferred to the blocking electrode and again we wait for (open-circuit) equilibrium to be achieved. In this new situation, $c_i(x)$ and σ_s will clearly assume values which lead to $\delta G = 0$ with $\delta\sigma_m = \delta\sigma_l = 0$. From the final, equilibrium charge values and distributions one can, at least in principle, calculate that ψ_m value, say ψ_{m3}, which is the equilibrium p.d. across the electrodes consistent with the total amount of charge which was passed to the blocking electrode while ψ_{m2} was applied. We assume that equilibrium was not reached during the application of ψ_{m2}; therefore, $|\psi_{m3}| < |\psi_{m2}|$. Now using a battery of proper voltage apply $\psi_{m1} = \psi_{m3}$ to the system as in the first situation. No current will flow and the charge distribution will remain unaltered. Hence, this final equilibrium state must be exactly the same as that which would have been reached if $\psi_m = \psi_{m3}$ had been applied continuously to the system. Thus, it is indeed consistent to take the variations of σ_m and σ_l zero even in the usual situation.

Equations (A14) and (A16) now lead immediately to

$$\begin{aligned} \delta G = \int_0^l \Bigg\{ &\left[\Delta G_1 + kT \ln\left\{\left(\frac{c_1(x)}{N - c_1(x)}\right)\left(\frac{\Gamma_s + (2\sigma_s/e)}{\Gamma_s - (2\sigma_s/e)}\right)\right\}\right. \\ &\left. - e(\psi(x) - \psi_s)\right]\delta c_1(x) \\ &+ \left[\Delta G_2 + kT \ln\left\{\left(\frac{c_2(x)}{2N - c_2(x)}\right)\left(\frac{\Gamma_s - (2\sigma_s/e)}{\Gamma_s + (2\sigma_s/e)}\right)\right\}\right. \\ &\left. + e(\psi(x) - \psi_s)\right]\delta c_2(x)\Bigg\} dx . \end{aligned} \tag{A17}$$

Now since $\delta c_i(x)$ may be arbitrary, one immediately finds the distributions given by Eq. (11) of the text when normalized potentials etc., are introduced. Thus we have shown that the same distributions are found in the present situation as those obtained by P–B, but with the electrode potential ultimately determining the value of the surface potential ψ_s in this case.

As is shown by one of us elsewhere,[49] the same distributions may be obtained from the assumption of local thermodynamic equilibrium if one makes use of the virtual chemical potentials for defect species introduced by

Kröger and Vink.[50] On defining the electrochemical potentials of the cation vacancies and interstitials as

$$\eta_1(x) = \Delta G_1 + kT \ln\{c_1(x)/[N - c_1(x)]\} - e\psi(x) \quad \text{(A18)}$$

and

$$\eta_2(x) = \Delta G_2 + kT \ln\{c_2(x)/[2N - c_2(x)]\} + e\psi(x) , \quad \text{(A19)}$$

respectively, and defining the electrochemical potential of the surface cations as

$$\eta_s = kT \ln\{\Gamma_2/(\Gamma_s - \Gamma_2)\} + e\psi_s \quad \text{(A20)}$$

one finds that the distributions of Eq. (11) are obtained directly from the requirements

$$\eta_1(x) + \eta_s = 0 \quad \text{(A21)}$$

and

$$\eta_2(x) = \eta_s \quad \text{(A22)}$$

when one makes use of the identity[5] $\sigma_s = e[\Gamma_2 - (\Gamma_s/2)]$. The above requirements are simply the thermal equilibrium conditions for the reactions

$$[\text{vacancy}] + [\text{surface cation}] \rightleftarrows 0$$

and

$$[\text{interstitial}] \rightleftarrows [\text{surface cation}] .$$

It should be noted that the activity terms in Eqs. (A18) and (A19) take full account of lattice statistics[9] [see Eq. (6)].

Finally, as in Eq. (25), one can obtain a first integral of Poisson's equation, now applicable to a fixed length l. In normalized terms the result is

$$[\phi'(X)]^2 - [\phi'(L)]^2 = \delta^{-1} \ln[1 + R_2(\phi)] , \quad \text{(A23)}$$

where $\phi(0) = \phi_d$, $\phi(L) = 0$, and $R_2(\phi)$ is given by Eqs. (26)–(28). Upon using Eqs. (A8) and (A23) with $X = 0$, then, in terms of normalized charge densities, one obtains

$$Q_m + Q_s = \mathrm{sgn}(\phi_d)\,[\delta^{-1} \ln\{1 + R_2(\phi_d)\} + Q_L^2\,]^{1/2} \equiv F_L(\phi_d, \delta) , \quad \text{(A24)}$$

where we have used $R_2(0) = 0$. Here $Q_L \equiv -\mathcal{E}_L \equiv \sigma_I/\sigma_n \equiv \phi'(L)$. Thus Q_L is the normalized charge density on the ohmic electrode. Since $Q_L \to 0$ as $L \to \infty$, the present $F_L \to F_\infty \equiv F$ in the same limit, where F is defined in Eq. (43). Now it follows from Eq. (A23) that

$$X = \int_{\phi}^{\phi_d} \frac{dY}{F_L(Y, \delta)} , \quad \text{(A25)}$$

and

$$L = \int_{0}^{\phi_d} \frac{dY}{F_L(Y, \delta)} , \quad \text{(A26)}$$

the latter an implicit equation for Q_L in terms of L, which shows that as $L \to \infty$ $|Q_L|$ becomes proportional to $\exp[-\{1 - (3\delta/4)\}^{1/2} L]$. The normalized differential capacitance of the material between $X = 0$ and L, C_{DON}, now made up of contributions from both the diffuse space charge region and the rest of the material, is finally given by

$$C_{DON} \equiv dF_I(\phi_d, \delta)/d\phi_d , \quad \text{(A27)}$$

where Q_L, of course, depends on ϕ_d as well as L.

APPENDIX B: GENERAL CAPACITANCE RELATIONS

For our general system, we may define the following normalized capacitances:

$$C_{DN} \equiv dQ_m/d\phi_m , \quad \text{(B1)}$$

$$C_{AN} \equiv -dQ_s/d\phi_s , \quad \text{(B2)}$$

and

$$C_{DON} \equiv -dQ_d/d\phi_d \equiv dF(\phi_d)/d\phi_d . \quad \text{(B3)}$$

We have already seen that in the absence of discreteness of charge effects, C_{AN} is given explicitly by Eq. (54). Further, C_{DON} is here the same normalized diffuse double layer capacitance as the C_{DN} calculated and discussed in Sec. IIC and IID except that the basic potential variable is here ϕ_d. Thus the earlier results for C_{DN} serve to illustrate some of the dependence of the present $C_{DON}(\phi_d)$ on its argument. Note that in the present case, if no surface charge can form and $C_\beta = C_\gamma = \infty$, i.e., the situation of an electrode immediately on the surface of the crystal with no inner layer separation, $C_{DN} = C_{DON}$.

It remains to obtain a general expression for C_{DN}. Using the above capacitance definitions, one finds that the operator $d/d\phi_m$ applied to Eq. (47) immediately yields

$$C_{DN} = C_{DON}\left(\frac{d\phi_d}{d\phi_m}\right) + C_{AN}\left(\frac{d\phi_s}{d\phi_m}\right) . \quad \text{(B4)}$$

Then, using (44) and (45), one can write

$$\frac{d\phi_s}{d\phi_m} = 1 - \lambda_\beta C_{DN} , \quad \text{(B5)}$$

$$\frac{d\phi_s}{d\phi_d} = 1 + \lambda_\gamma C_{DON} ; \quad \text{(B6)}$$

and thus

$$\frac{d\phi_d}{d\phi_m} = \left(\frac{d\phi_d}{d\phi_s}\right)\left(\frac{d\phi_s}{d\phi_m}\right) = \left(\frac{1 - \lambda_\beta C_{DN}}{1 + \lambda_\gamma C_{DON}}\right) . \quad \text{(B7)}$$

Now from (B4), (B5), and (B7) it follows, on solving for C_{DN}, that

$$C_{DN} = \frac{C_{DON} + [1 + \lambda_\gamma C_{DON}]C_{AN}}{1 + (\lambda_\beta + \lambda_\gamma)C_{DON} + \lambda_\beta[1 + \lambda_\gamma C_{DON}]C_{AN}} , \quad \text{(B8)}$$

or

$$C_{DN} = \frac{1 + [\lambda_\gamma + C_{DON}^{-1}]C_{AN}}{(\lambda_\beta + \lambda_\gamma) + C_{DON}^{-1} + \lambda_\beta[\lambda_\gamma + C_{DON}^{-1}]C_{AN}} . \quad \text{(B8')}$$

The last form is useful when the diffuse double layer is so dense that C_{DON}^{-1} may be neglected compared to $\lambda_\gamma \equiv C_{\gamma N}^{-1}$. As far as we are aware, these general expressions have not been given previously.

On differentiating Eq. (43), one finds

$$C_{DN} = C_{DON}\left(\frac{d\phi_d}{d\phi_m}\right) - \frac{dQ_s}{d\phi_m} , \quad \text{(B9)}$$

which becomes, on using (B7) and solving for C_{DN}:

$$C_{DN} = \frac{C_{DON}}{1 + (\lambda_\beta + \lambda_\gamma)C_{DON}} - \left(\frac{1 + \lambda_\gamma C_{DON}}{1 + (\lambda_\beta + \lambda_\gamma)C_{DON}}\right)\frac{dQ_s}{d\phi_m} . \quad \text{(B10)}$$

Now write $(dQ_s/d\phi_m) = C_{DN}(dQ_s/dQ_m)$ and solve for C_{DN}^{-1}, obtaining

$$C_{DN}^{-1} = (\lambda_\beta + \lambda_\gamma) + C_{DON}^{-1}\left(1 + \frac{dQ_s}{dQ_m}\right) + \lambda_\gamma \frac{dQ_s}{dQ_m}$$

$$= C_{\beta\gamma N}^{-1} + C_{DON}^{-1} + (C_{\gamma N}^{-1} + C_{DON}^{-1})\frac{dQ_s}{dQ_m} , \qquad \text{(B11)}$$

where $C_{\beta\gamma N}^{-1} \equiv \lambda_\beta + \lambda_\gamma \equiv (C_{\beta N}^{-1} + C_{\gamma N}^{-1})$. An expression equivalent to (B11) was first given by Devanathan.[35] It has also been used by Bockris and Reddy[36] for a concentrated aqueous electrolyte where C_{DON}^{-1} was taken very small and neglected. Equation (B11) is interesting but may be potentially misleading. Bockris and Reddy have calculated dQ_s/dQ_m separately (see Refs. 24, 37, and 38 for rather stringent criticisms of their approach, which is based on earlier work of Bockris, Devanathan, and Muller) and used the result in their equivalent of Eq. (B11) to obtain C_{DN}. But it is readily shown from the present equations that

$$\frac{dQ_s}{dQ_m} = [\lambda_\beta - C_{DN}^{-1}]C_{AN} ; \qquad \text{(B12)}$$

thus, a complete treatment would require the substitution of (B12) in (B11) and solution for C_{DN}, yielding a result in agreement with the exact expression of (B8). By not carrying through this last step, one fails to obtain (B8) and the simple equivalent circuit with which it is consistent.

[1]J. Frenkel, *Kinetic Theory of Liquids* (Oxford University, New York, 1946), pp. 36–40.
[2]T. B. Grimley, Proc. R. Soc. (London) Ser. A 201, 40 (1950).
[3]K. L. Kliewer and J. S. Koehler, Phys. Rev. 140A, 1226 (1965).
[4]K. L. Kliewer, J. Phys. Chem. Solids 27, 705 (1965).
[5]R. B. Poeppel and J. M. Blakely, Surf. Sci. 15, 507 (1969).
[6]D. O. Raleigh, Phys. Status Solidi A 4, 215 (1971).
[7]J. M. Blakely and S. Danyluk, Surf. Sci. 40, 37 (1973).
[8]J. R. Macdonald, J. Appl. Phys. 45, 73 (1973).
[9]A. T. Fromhold, *Theory of Metal Oxidation*, Vol. I (North Holland, Amsterdam, 1976), pp. 40ff.
[10]J. R. Macdonald and M. K. Brachman, J. Chem. Phys. 22, 1314 (1954).
[11]G. Gouy, J. Phys. Radium 9, 457 (1910).
[12]S. Danyluk and J. M. Blakely, Surf. Sci. 41, 359 (1974).
[13]W. Weppner and R. A. Huggins, Ann. Rev. Mat. Sci. 8, 269 (1978).
[14]J. R. Macdonald, J. Chem. Phys. 58, 4982 (1973).
[15]Reference 9, p. 121.
[16]P. Delahay, *Double Layer and Electrode Kinetics* (Interscience, New York, 1965), pp. 81ff.
[17]A. Clark, *The Theory of Adsorption and Catalysis* (Academic, New York, 1970), pp. 17ff.
[18]R. de Levie, J. Electroanal. Chem. 82, 361 (1977).
[19]H. U. Beyeler and S. Strässler, Phys. Rev. B 20, 1980 (1979).
[20]S. M. Sze, *Physics of Semiconductor Devices* (Wiley, New York, 1969), p. 90.
[21]J. Corish and P. W. M. Jacobs, J. Phys. Chem. Solids 33, 1799 (1972).
[22]R. J. Friauf, J. Phys. (Paris) 38, 1077 (1977).
[23]D. O. Raleigh, Electroanal. Chem. 6, 87 (1973).
[24]C. A. Barlow, Jr. and J. R. Macdonald, Adv. Electrochem. Electrochem. Eng. 6, 1 (1967).
[25]E. Gileadi, in *Electrosorption*, edited by E. Gileadi (Plenum, New York, 1967).
[26]J. R. Macdonald and C. A. Barlow, Jr., J. Chem. Phys. 39, 412 (1963).
[27]J. R. Macdonald and C. A. Barlow, Jr., in *Electrochemistry*, edited by A. Friend and F. Gutmann (Pergamon, Oxford, 1965).
[28]J. O'M. Bockris and A. K. N. Reddy, *Modern Electrochemistry*, Vol. II (Plenum, New York, 1970), pp. 756–757.
[29]R. D. Armstrong, T. Dickinson, W. P. Race, and R. Whitfield, J. Electroanal. Chem. 27, 158 (1970).
[30]J. R. Macdonald and C. A. Barlow, Jr., J. Chem. Phys. 44, 202 (1966).
[31]C. Mead, Phys. Rev. Lett. 6, 545 (1961).
[32]J. R. Macdonald, J. Appl. Phys. 35, 3053 (1964).
[33]R. D. Armstrong, J. Electroanal. Chem. 52, 413 (1974).
[34]F. Trautweiler, Photogr. Sci. Eng. 12, 98 (1968).
[35]M. A. V. Devanathan, Trans. Faraday Soc. 50, 373 (1954).
[36]Reference 28, pp. 750–752.
[37]C. A. Barlow, Jr. and J. R. Macdonald, J. Chem. Phys. 43, 2575 (1965).
[38]R. M. Reeves, in *Modern Aspects of Electrochemistry*, Vol. 9, edited by B. E. Conway and J. O'M. Bockris (Plenum, New York, 1974).
[39]R. Parsons, J. Electroanal. Chem. 5, 397 (1963).
[40]J. R. Macdonald, in *Electrode Processes in Solid Ionics*, edited by M. Kleitz and J. Dupuy (D. Reidel, Dordrecht-Holland, 1976).
[41]S. G. Davison and J. D. Levine, in *Solid State Physics*, Vol. 25, edited by H. Ehrenreich, F. Seitz, and D. Turnbull (Academic, New York, 1970).
[42]Reference 28, pp. 762–769.
[43]J. R. Macdonald and D. R. Franceschetti, J. Chem. Phys. 68, 1614 (1978).
[44]E. Gileadi, E. Kirowa-Eisner, and J. Penciner, *Interfacial Electrochemistry* (Addison–Wesley, Reading, Mass., 1975), p. 87.
[45]Reference 28, pp. 740–741, 748–749.
[46]R. Fowler and E. A. Guggenheim, *Statistical Thermodynamics* (Cambridge University, Cambridge, 1949), p. 544.
[47]M. Abraham and R. Becker, *The Classical Theory of Electricity and Magnetism* (Hafner, New York, 1950), pp. 233–235.
[48]H. Goldstein, *Classical Mechanics* (Addison–Welsey, Reading, Mass., 1965), p. 33.
[49]D. R. Franceschetti, submitted to Solid State Ion.
[50]F. A. Kröger and H. Vink, Solid State Phys. 3, 307 (1956).